REVIEW

# A Critical Analysis of the Tensile Adhesion Test for Thermally Sprayed Coatings

Shalaka Shinde[1] · Sanjay Sampath[1]

**Abstract** Tensile adhesion tests (TATs) are an economical and convenient tool to assess the bond strength of thermal spray coatings and provide insight into manufacturing reliability and potentially component performance in service. It is a common practice to employ the TAT as per the recommendations outlined in various standards like ASTM C633 or ISO 14196. The industry accepts the TAT results as a characterizing parameter of coating adhesion. Although widely used for decades, the fundamental aspects of this test concerning its fidelity and reliability, relevance to bonding mechanisms, linkage to performance in service, and their material/substrate parametric dependencies are significantly limited. This work critically examines the test attributes, specimen preparation, material responses, reliability, and processing linkages through a comprehensive assessment of literature data and industrial practices along with carefully designed in-house experiments (where necessary to sort through inconsistencies in the literature) on a range of coating-substrate systems and processes. This assessment points to several challenges in accepting available data, especially regarding a lack of definition of failure loci and widespread variability in test results. It is noted that variability can arise from testing practices (specimen geometry, edge effects, etc.) and intrinsic material attributes primarily for brittle coatings (flaw variations at the interface and associated toughness issues). The integrated results and analysis presented in this paper suggest that the test is intrinsically variable and highly sensitive to testing nuances and flaws (especially in ceramics), leading to inconclusive outcomes. In non-brittle systems (metals and carbides), the test evaluates the strength of the interface, with possible linkages to operative mechanisms of adhesion. It is envisioned that these developments, along with more robust descriptions of processing-related attributes (residual stresses, modulus, etc.), will enable further refinement of the method along with innovations for more advanced measurements.

**Keywords** adhesion strength · bond strength · ceramic coatings · elastic modulus · fracture toughness · residual stresses · roughness · tensile adhesion test

**Abbreviations**

| | |
|---|---|
| Al | Aluminum 6061 substrate |
| AlBr | Aluminum (9%) bronze |
| APS | Air plasma spray |
| ASTM | American society for testing and materials |
| CrC-NiCr | Chrome carbide nickel chrome cermet |
| CS | Cold spray |
| DVC | Segmented or dense vertically cracked coatings |
| HVOF | High-velocity oxy-fuel |
| ISO | International organization for standardization |
| Ni | Nickel |
| Ni-5Al | Nickle-5% aluminum |
| St | Low carbon steel substrate |
| T400 | Commercial cobalt alloy, Tribaloy T-400 |
| T800 | Commercial cobalt alloy, Tribaloy T-800 |
| TAT | Tensile adhesion test |
| TWA | Twin wire arc |

✉ Shalaka Shinde
shalaka.shinde@stonybrook.edu

1　Center for Thermal Spray Research, Stony Brook University, Stony Brook, NY, USA

WC–Co    Tungsten carbide-cobalt cermet
YSZ       Yttria-stabilized zirconia

## Introduction

Thermal spray deposition of solid feedstock material is a widely established materials processing technology used across various industries. (Ref 1-14). Thermal spray processes (Ref 15-17) are very versatile and are used to fabricate coatings using ceramics, metals, multicomponent alloys, and cermets (Ref 18). In general, thermal spray coatings build up incrementally from individual particles that impact and adhere to the substrate. These individual impacted particles that serve as the building blocks of the coating are commonly known as 'splats.' The interaction between the splats and the underlying substrate (or the previously deposited particles/layers) is influenced by the impinging particle properties—for instance, the temperature, velocity, particle/droplet size, and the phase (liquid, partially liquid, etc.) (Ref 19-21). Because of such unique formation dynamics, the resulting coating properties are governed by the bonding quality between the deposited coating material and the substrate.

In the evolution of thermal spray coatings and their applications, one of the central themes for strategic innovations has been the optimization of the adherence quality at the interface between the substrate and the coating (Ref 22, 23). Therefore, investigating the mechanisms of adherence of the coating/substrate interface, either qualitatively or quantitatively, has been pursued concurrently in both academic and industrial research for decades. As a result of these efforts, in many industrial coating applications, a quantitative measure of adhesion is part of the coating qualifying specifications. Consequentially, the measurement and reporting of adhesion are almost universally adopted by thermal spray operations worldwide.

Despite the widespread acceptance and use, both the concept of coating adhesion strength in terms of its relation to the manufacturing process; and how it can be implemented into coating design remains an enigma. The purpose of this article is to present the reader with a comprehensive and critical analysis of the TAT. This article is intended for a wide range of audiences–from those new to adhesion strength evaluation in thermal spray coatings to those well-versed in the technique and methodologies.

This article is organized to provide a combination of relevant historical published data and industrially acquired large production data sets measured to meet specifications (unpublished but based on industry best practices). The article further phenomenologically breaks down the test fundamentals, standards/guidelines, and materials/process sensitivities. Due to a lack of clarity in the literature data to capture the phenomenological nuances, wherever necessary, 'in-house' experiments were conducted to provide additional insights. This combined approach allowed rationalizing of the testing protocols enabling a common platform for future comparisons. Lastly, the paper synthesizes the results through notional process maps based on the classification of flaw-dominant responses in brittle ceramics, along with a discussion of parametric factors that affect operative mechanisms in metallic and cermet systems.

## Adhesion Fundamentals

The interface between two materials in contact with each other is characterized by the amount of energy required to create free surfaces from the bonded region; this energy term is conceptually referred to as the 'True Work of Adhesion' (Ref 24). It is an intrinsic property of the bimaterial pair and is affected by the type (or mechanism) of bonding between them (i.e., mechanical interlocking, chemical bonding, physical adsorption, etc.) as well as the level of initial surface contamination prior to mating the two materials. The True Work of Adhesion—under ideal Mode I Griffith Fracture (Ref 25) is mathematically equivalent to the interfacial toughness (i.e., the energy required to drive a delamination crack along the substrate/coating interface).

However, experimental measurement of the true work of adhesion in natural systems is extremely challenging. The major issue in measuring the work of adhesion is accurately quantifying work done in debonding the materials along the interface. This is because, in most practical systems, the work required to debond materials will inevitably contribute to frictional losses and plastic deformation (Ref 24). These energetic losses cannot easily be decoupled from experimental measurements of interfacial strength. Thus, the scope of testing for true work of adhesion is limited, and the use of this thermodynamic definition in high-volume industrial settings is not feasible. Hence, several alternative test methods have been developed to compare the interface quality of coatings and impose coating quality control/specification limits (Ref 26).

There are over 200 adaptations of the adhesion tests used to characterize the quality of an interface (Ref 24, 26-29), and discussion on the individual advantages and challenges of each adaptation is beyond the scope of this article. However, the central theme in all such tests is to empirically "infer" the interface quality by subjecting a representative specimen to some external load and measuring the critical value at which delamination occurs. From these adaptations, it has become a common industrial

practice to develop/employ a coating specification that cites a particular threshold value of "adhesion strength" that a coating (or test specimen) must exceed to pass qualification (Ref 30-32).

One of the most convenient and widely adopted methodologies to assess the quality of interfacial bonding (especially for thermal spray coatings) is known as the 'Tensile Adhesion Test' (TAT, also known as 'Adhesion Strength' or 'Bond Strength' test). TATs are popular in original equipment manufacturers (OEMs) and overhaul sites due to several important factors such as the ease of use, economical consumables, low maintenance equipment, and compatibility among various coating processes. Therefore, many thermal spray industries actively use this test as a qualification tool.

The subsequent sections in this review article are dedicated to presenting a comprehensive overview of the development, adoption, and contemporary understanding of the TAT as it has evolved over the decades. The main questions that are addressed in the article are:

i. What common variations are observed in procedural approaches implemented at TAT testing sites?
ii. What are sources of variability in the adhesion strength measurements?
iii. How does the microstructural quality of the coating relate to the adhesion strength of the interface?
iv. Why is it challenging to integrate the established cause–effect relations from TAT results into one universally applicable (to multiple coating-substrate systems obtained via different materials and/or thermal spray processes) mechanism and/or theory?

### Tensile Adhesion Test (TAT)

TAT determines the degree of adhesion of a coating–substrate interface by measuring the tensile load required to induce failure at the interface (in other words, to debond the coating from the substrate) (Ref 33).

In this test, a specimen compatible with the tensile loading equipment must be utilized. Typically, two dimensionally equivalent substrates are used to assemble a TAT specimen and identified as the coated or mating piece. The coating is first deposited on one of the two substrates. Before deposition, the substrate surface is grit-blasted/roughened to a representative surface roughness condition of the actual component in service. Then, the coating is bonded to the mating piece with the help of glue (or adhesive). Once properly glued/cured, the assembly is subjected to a uniaxial tensile load, perpendicularly applied to the plane of the coating–substrate interface until failure occurs. It is necessary for a conclusive/successful test that the coating entirely debonds from the substrate during this

test. For such interfacial separation, the 'Adhesion Strength' or 'Bond Strength' of the coating–substrate interface is reported as:

$$\text{Adhesion Strength[MPa or ksi]} = \frac{\text{Tensile Load at Failure}}{\text{Cross} - \text{Sectional Area}}$$

(Eq 1)

All other plausible results for a TAT are illustrated schematically in Fig. 1. Note that there are alternative definitions for the measured strength based on the plane of separation in the system after the failure occurs. For instance, if the delamination takes place entirely along a plane contained within the coating, the results are reported as the 'Cohesive Strength of the coating'. In multilayered samples, the sample could also fail along the boundary of the two discrete layers. In such cases, the failure is categorized as an "internal adhesive" failure (Ref 34, 35).

When the fracture occurs entirely within the glue layer, no information regarding the interface or coating is gained. However, the interface and the coating strength can be concluded to be greater than the bonding strength of the glue itself, assuming the glue did not infiltrate the coating. Such "glue failures" are commonly observed in high-quality High-Velocity Oxy-Fuel (HVOF) cermet coatings. Therefore, obtaining a glue failure in an HVOF TAT specimen has become an accepted practice to qualify a coating. If the failure occurs in some combination of different locations (partially along the interface and/or within coating), then such test is declared "inconclusive."

While Fig. 1 schematically provides a baseline for defining an acceptable fracture surface, note that the criterion for determining whether a TAT is conclusive has a significant operator/site bias. To mitigate these ambiguities, one of the testing protocols known as the ISO:14,916 standard (Ref 34) recommends the user to quote the respective areas in the order of magnitude (e.g., 90/10% adhesive/cohesive), which can help in establishing unbiased interpretation across multiple sites.

Because the primary focus of this article is restricted to the discussion of the historical and contemporary characterization of interfaces and interfacial strengths, the results presented are constrained only to the adhesion strengths. This data compilation methodology also justifies the need for further experimental work to fill the "knowledge gaps" for which the available literature data do not satisfy this criterion.

### Historical Evolution of TAT

The TAT (in all its archetypes) has been in practice for thermal spray coatings for more than five decades. One of the first published standard protocols for a tensile test can be found in the ASTM C633-69 standard. The standard was
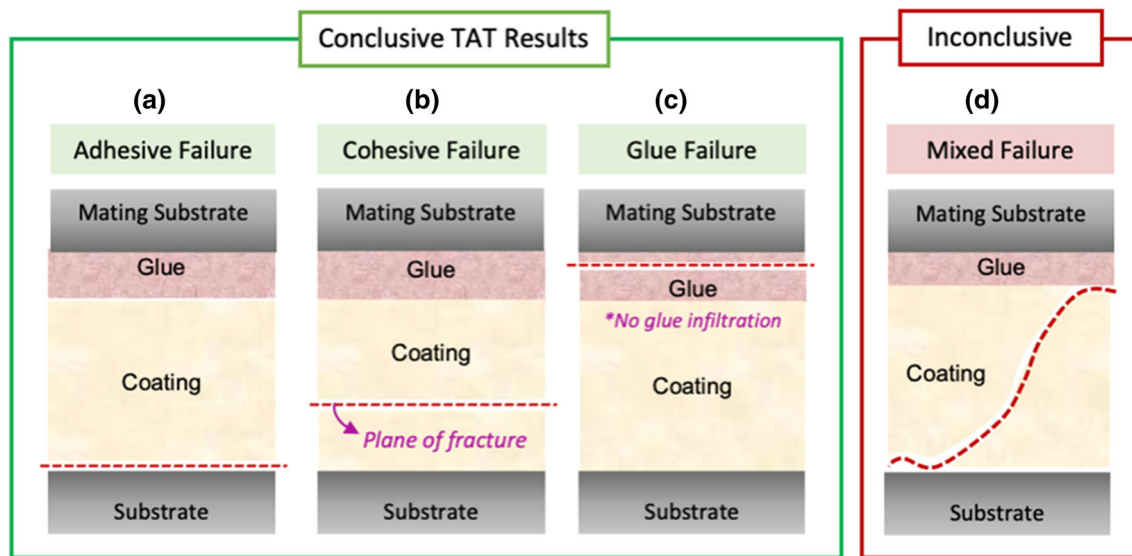
**Fig. 1** A schematic representation of typical paths of separation observed in a TAT bilayer sample after failure that is representative of a successful (a) adhesive, (b)cohesive, (c) glue failure, or (d) an inconclusive test showing mixed or partial separation

initially limited to characterizing flame-sprayed coatings. Later, a compilation of 25 papers was put together by Mittal (Ref 36) in 1978 that developed a generic set of protocols for determining the adhesive features of thin films, thick films, and bulk coatings. In 1983, the ASTM C633 standard was revised to be utilized for an extended set of thermally sprayed coatings (i.e., those fabricated using multiple processes). The ASTM C633 standard is subjected to an internal review for updates every five years. The contents of the most recent revision of the standard were published in 2013 and reapproved in 2017 and 2021. It is accepted practice to cite an ASTM C633 standard, modify the methodology to suit specific experimental needs, and outline what procedural deviations from the ASTM were taken in the publication.

Independent of the ASTM C633 standard, several other procedures exist to determine the adhesion strength for thermally sprayed coatings. Historical mentions for documents from regional databases of France (Ref 37), Germany (Ref 38), and Japan (Ref 39) are available in the literature (Ref 33, 40, 41). However, some of these documents were annulled or superseded over the years. Discussion on the differences between all archetypes of the historical standards is beyond the scope of this article.

At present, apart from the ASTM C633-13 (2021) (Ref 35), other popular adhesion testing standards in practice include the DIN EN ISO 14916 standard, which was revised in 2017–18 (Ref 34), and the JIS H 8402 standard published in 2004 (Ref 42). The Japanese Standards Association (JSA) commented that the JIS H 8402 document is the same as the ISO 14916 standard (Ref 42). Detailed comparative analysis of the most current ISO

14916: 2017 and ASTM C633:2013 is presented in Table 1.

This article will primarily focus on the implementation, applicability, and reproducibility of the ASTM C633 methodology.

## Contemporary Assessment and Interpretation of ASTM Test

Since its inception, TAT has been frequently implemented in the industry for two purposes. First, to establish a sense of reliability (i.e., how does one compare coatings from different deposition batches/lots). Second, to develop an understanding of performance (i.e., how does one quantify how good the coating-substrate interface may be).

Because of years of adoption, testing, and fabrication, a notional trend in TAT results has emerged within the thermal spray community, wherein the combination of coating fabrication processes and the subsequently incorporated porosities are related to the coatings' nominal adhesion strength. This is introduced schematically in Fig. 2, based on the range of typical adhesion strength values reported in the published literature (Ref 17, 41, 43-50). For illustrative reference, the typical range for two popular types of glue: FM1000 wafers (Ref 51) and semi-solid gel-based glues, is shown in the plot.

A notional map such as Fig. 2 indirectly draws attention to the properties of the incoming particles (droplets/splats) and the qualitative character of their interaction with the substrate. The most notable inherent factor here is the trend represented in Fig. 2–wherein the velocity of the incoming splats before impact influences the coatings' adhesion

**Table 1** Comparison between the recommended TAT testing guidelines from two independently operational standards ASTM C633-13 (Reapproved in 2021) and ISO 14916 (2017)

| | ASTM C633:13 [35] (Reapproved 2021) | ISO 14916: 2017 [34] |
|---|---|---|
| **Differences** | | |
| Substrate Geometry | Substrate Block (Rod geometry) | Substrate Block (Rod geometry) Test Disc (7 mm) |
| Substrate Diameter | Between 23 to 25.4 mm | 25 mm Or 25.4 mm Or 40 mm |
| Substrate Material | Preferably metal intended for use as the substrate for coating Or SAE 1018/1020 steel | Materials with comparable strength or chemical and physical properties |
| Substrate Length | $\geq 38.1mm$ | $\geq 50mm$ |
| Coating Thickness | $> 380\mu m$ | $> 80\mu m$ |
| No of Samples | $\geq 5$ | $\geq 3$ |
| Recommended Adhesives | FM 1000 M666 Armstrong A-12 Epoxy Adhesive EC-2214 | No specific suggestions |
| **Similarities** | | |
| Testing control rate | Position controlled Between $0.013 to 0.021mm/sec$ (ASTM) or equivalently $0.017\pm 0.004mm/sec$(ISO 14916) | |
| Test Requirement | Tensile test is conducted at room temperature such that: i.Equipment is self-aligning or allows self-alignment ii.Each sample is subject to uniaxial tension (without bending or torque) | |
| Reference Specimen | Glue sample is tested with every set as a control for: i.Quality of glue (monitoring deterioration with shelf life) ii.Consistency in the sample preparation method | |
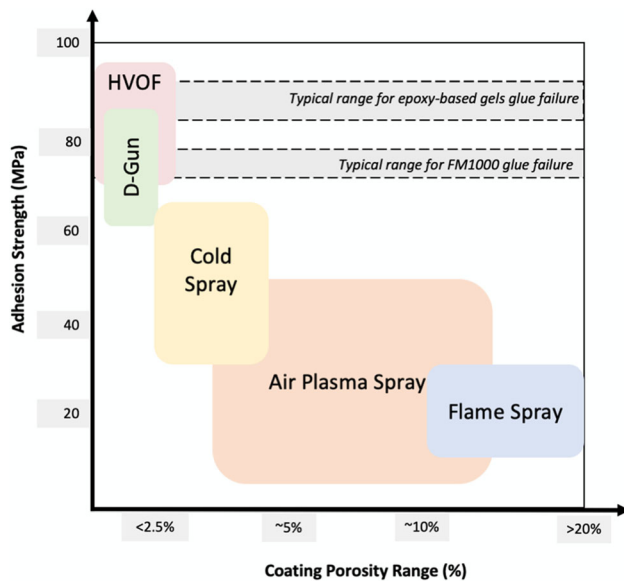
**Fig. 2** A conceptual understanding of the tensile adhesion strength of the coatings in relation to the empirically observed porosities in different thermal spray processes. The plot is based on data extracted from referenced sources (Ref 17, 27, 33) and should be taken for contextual representation

strength. As will be shown in the discussion, this approach is simplistic and does not account for material attributes (flaw tolerance) and test variabilities.

## Challenges and Limitations in Reconciling Published TAT Data

The traditional school of thought that has evolved with the widespread use of TAT in the thermal spray community dictates that if the standard guidelines are stringently followed, one can readily establish a consistent and reproducible adhesion strength for a system. In addition, although it has been shown that multiple adhesion strength standards are readily available, there is no universally followed testing procedure for conducting a TAT.

The standards provide preliminary guidelines—mainly centered around two themes: Sample preparation (dealing with substrate geometry, dimensions, and material recommendation) and Testing Method (elaborating on loading rates and the number of samples for the test). The critical shortcomings of the existing literature and current practices on TATs include:

i.  The guidelines in the standards have evolved over the years, along with significant deviations in the design of the accessories used in measurements (i.e., fixturing, adhesive choices, substrate geometries, tensile machines, and the capacity and sensitivity of modern load cells, etc.). Therefore, the backward compatibility of the data is limited.

ii.  Industrial sites often take an "adopted" approach, wherein the methods of the standards are individualized based on the site/operator, and diversions are stipulated in reporting.

iii.  The published TAT data are often gathered from a relatively small number of tested samples (population size) of 3–5 samples for a given coating-substrate combination. Numerous studies have pointed out that understanding the trends in adhesion strength responses can only be reliably understood via statistical analysis of a large sample set (Ref 28, 52, 53).

Thus, despite the vast adoption in industrial and academic research, publicly available TAT results fail to provide an *unbiased pool of unanimously accepted, statistically reliable data*. Thus, isolating the critical factors that determine the adhesion strength of interfaces has been a leading challenge for the community. Data available in existing literature thus cannot be easily reconciled to establish reliable unilateral trends across multiple material systems. This indicates the need for an extensive self-consistent dataset with high fidelity. Therefore, considering the lack of available literature in this specific domain, it was necessary to generate in-house data to address concerns where appropriate.

The current work aims to collect and assess results from the literature, industrially generated data, and in-house data. Including the in-house data in the article attempts to bridge the gap in published literature where the procedure and failure locations are not clearly identified or unavailable. To facilitate systematic documentation of all the in-house experiments, the generic experimental methods for spraying, preparing, and testing TAT specimens are provided in the Appendix A1 and A2 of this review.

Sections "Sample Assembly of TAT: Accepted Practices" and "Interface Attributes in Tensile Adhesion Test" in this article provide a detailed overview of the influence of sample assembly and the interface attributes on TAT results and how these aspects can influence the variability in measured outcomes. Section "Discussion" finally presents a reconciled synthesis of all the results in this article and strives to discuss future research directions in studying the adhesion of thermally sprayed coatings at interfaces.

## Sample Assembly of TAT: Accepted Practices

The results of investigations toward quantifying the effect of testing practices on TAT variability are presented here in three subsections: Deposition Considerations (substrate geometry and edge), Preparation Procedure (glue

properties and post-curing issues), and Testing Methodology (test control and the number of samples).

## Effect of Deposition Attributes

### Substrate Geometry

There are two available choices for substrate geometry in TATs. One of the geometries involves grit blasting a TAT-ready substrate (i.e., a rod) and spraying directly onto the roughened substrate surface. Once sprayed, the coated specimen is glued to another grit-blasted TAT-ready substrate yielding a dimensionally symmetric specimen. This configuration will be hereafter referred to as the Rod Geometry and is illustrated in Fig. 3.

It is common in industrial practice to tack weld small discs/coupons onto complex components during deposition. Alternatively, coupons can be sprayed on an independent setup while mimicking the part deposition parameters. Such coupons are traditionally used as "witness" disks/coupons for microstructural investigations or as TAT specimens. In TAT sample geometry involving witness coupons, the sprayed disk is glued onto two mating substrates (using two layers of glue). The schematic presentation is shown in Fig. 3 and will be referred to as the Disk Geometry hereafter. The ASTM recommends using Rod geometry, whereas the ISO 14916 standard accepts both geometries (See Table 1).

The available literature on studies that specifically investigate the difference between the rod vs. disk geometries is limited. Hence in this work, experiments were conducted in-house to benchmark the differences. Equivalent APS Yttria-Stabilized Zirconia (YSZ) coatings were deposited on Aluminum 6061 substrates of the two specimen geometries shown and tested. The substrates in rod geometry were 1.5 inches (38.1 mm) long with a diameter of 1 inch (25.4 mm) (in agreement with the ASTM C633 standard). The disks used were also 1 inch (25.4 mm) in diameter; however, the thickness was only 0.25 inches (6.25 mm). The TAT results indicate that both the samples failed in 100% adhesion. Elaborated experimental details are outlined in Appendix A1.

Figure 3 suggests that the disk geometry had a higher adhesion strength than the rod geometry. Although the exact cause for such a dramatic increase in adhesion strength cannot be isolated based on results from a single experiment, the results indicate the need for a rigorous inquiry. Specifically, two potential sources can affect the
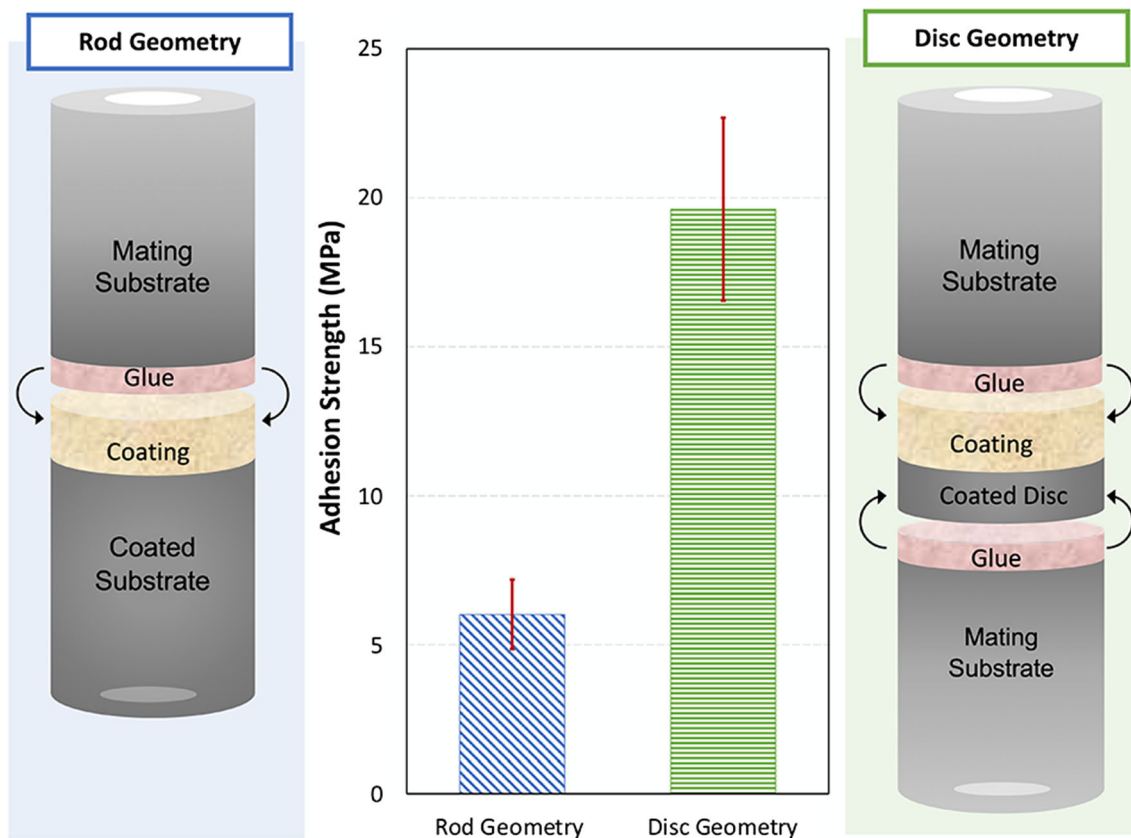


**Fig. 3** Two of the most common TAT substrate geometries: rod (aluminum) and aluminum disk (assembled with steel rods), with a relative comparison of adhesion strength obtained by testing equivalent YSZ coatings on aluminum substrate

stress at the interface: testing geometry and the process-induced attributes. Process-induced attributes include microstructural differences due to variations in thermal history during deposition and the residual thermal stresses in the system. Reports by Han et al. (Ref 54, 55) have pointed out that the interface's stress depends on the substrate dimensions.

Preliminary finite element analysis suggests that the stress at the interface in the rod geometry is lower than that of the Disc-geometry when subjected to identical displacement conditions. This indicates that the observed results in adhesion strength of in-house samples tested with the two geometries primarily arise from process-induced stress differences at the interface.

The results warrant dedicated investigation that has not been yet accomplished in the literature or as a part of this work. Although the current state of analysis on these results fails to explain the observed differences, it suffices to highlight that dramatic discrepancy can be expected in the adhesion strength analysis due to the test geometries.

It is also evident that comparing adhesion data from two geometries is inappropriate as they represent two different tests. Furthermore, this result points to another issue: the adhesion results are highly dependent on the system.

### Substrate Edges

Substrates with sharp edges are recommended for adhesion strength tests (Ref 34, 35). However, most practical substrates in thermal spray are chamfered or rounded to some extent. For instance, most industrial sites will use commercially available pre-machined discs/rods due to their availability, ease of handling, and manufacturing cost. In addition, substrate edges can deform during deposition with thermal spray processes that induce high peening stresses (such as HVOF and Cold Spray).

Again, the literature does not provide many results from specifically dedicated studies that address the effect of edge-rounding on the adhesion strength of thermally sprayed systems. However, some studies report that the substrate geometric features can affect the stress distribution at the interface (Ref 54, 55). As a result, samples of deliberately different substrate geometry were fabricated and tested by the authors to assess the significance of the geometry of the substrate edge.

Figure 4 compares the experimentally measured adhesion strength results for equivalently sprayed APS YSZ coatings ($\sim 450~\mu m$ thick) deposited on steel rod TAT substrates with a sharp (no chamfer) and chamfered edge (chamfer $\sim 6.35~mm$). It was observed that both samples had 100% adhesive failure. Although there is a subtle indication that chamfer might help reduce stress intensity at the edge, the scatter in the data hinders the deduction of
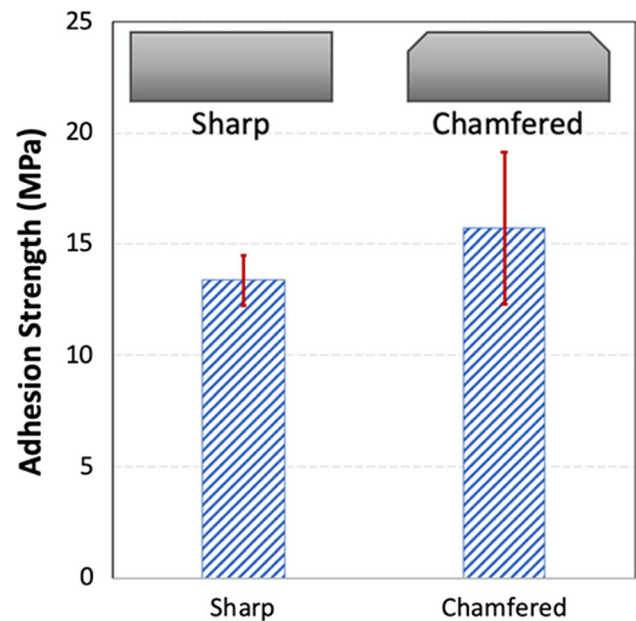


**Fig. 4** Comparison adhesion strength of APS YSZ/Steel interfaces as measured with Rod Geometry specimens with sharp and chamfered edges, respectively. All samples failed in 100% adhesion

any conclusive correlation in the results. Furthermore, comprehensive work incorporating modeling needs to be considered.

In addition to testing samples manufactured with a pre-made chamfer, there was equal interest in understanding the effect of re-using substrates. Thus, an in-house experiment was conducted with new sharp rods and reused rods deposited with equivalent APS YSZ coatings (Fig. 5). In this study, specimens were pressure-blasted (a different procedure from grit blasting) at 4.13–5.51 bar with #24-grit alumina to remove/strip the coating and leftover glue residue mechanically. Then the pressure-blasted specimens were re-grit blasted, and the roughness was evaluated with a profilometer to verify the surface roughness ($R_a$) between a brand-new grit-blasted rod and the re-grit-blasted rod are equivalent.

As shown in Fig. 5(b), the average adhesion strength was observed to increase in the case of the reused/re-grit-blasted rod substrates by $\sim 21\%$, with a larger scatter in the data. The equivalency of slopes in the raw load–displacement curves (Fig. 5c, d) implies that both new and reused substrates had a mechanistically similar response to the applied load. However, like the chamfered rods, the reused substrates do not substantially alter the adhesion strength. This is a significant result, as it is often economical and common to re-use TAT substrates in a high-throughput industrial environment.
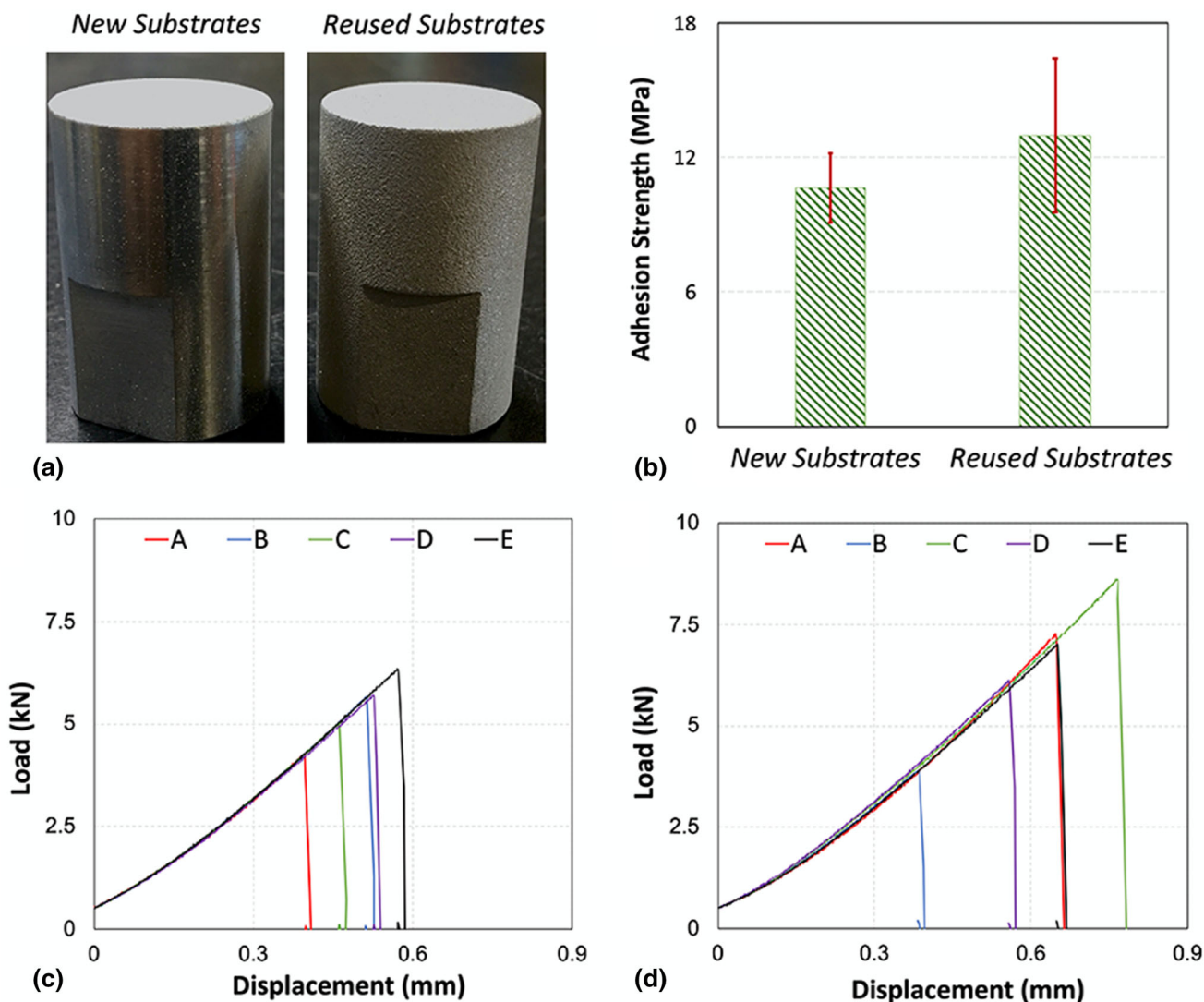
(a)

(b)

(c)

(d)

Fig. 5 Comparison between APS YSZ/Aluminum interfaces assembled with new, sharp aluminum rod substrates and reused substrates: (a) pictures of sample substrates (b)Average adhesion strength data sampled over 5 specimens (labeled A-E). Raw load–displacement data for (c) new and (d) reused substrates indicates the consistency in slopes for both the samples. All samples failed 100% adhesively

## Influence of Glue (Adhesive) and Curing Attributes

The primary design metric of a suitable glue to be used in a TAT experiment is centered around two major requirements: First, the glue must exhibit higher strength than the intended interface to be tested (to allow the possibility for the system to fail adhesively at the interface). Second, the glue should neither interact nor infiltrate the coating, as it can potentially influence the test results (Ref 34, 35). This is especially important for porous coatings, where capillary infiltration can occur.

Numerous commercially available adhesives meet the criteria above and have been widely used for TATs. Unlike the active ISO 14916 standard, the ASTM C633 standard suggests some glues for users to consider (See Table 1). During the evolution of the TAT in the past few years, two

glue compositions have gained ubiquitous popularity in the thermal spray community. They are known among users as the FM1000 Wafers (polyamide epoxy composition) [Sturbridge Metallurgical Services, Inc., MA] and the thermoset epoxy resin gel MasterBond [MasterBond EP-15ND, MasterBond Inc., NJ]. While MasterBond does indeed yield higher adhesion strengths, the FM1000 wafers offer an easy, reliable, and consistent/reproducible glue layer for TATs. Thus, FM1000 is widely recognized to be more suitable for large-scale industrial testing. Table 2 provides a brief overview of their properties.

One limitation of both MasterBond and FM1000 is that they are thermally cured epoxy glues. When using heat-cured glues, the loss of viscosity of the glue during the heat treatment for curing is inevitable. With a decrease in the viscosity, the propensity of the glue to infiltrate the coating

**Table 2** A Comparison between the commercially popular glue (adhesives) used in TATs based on the *manufacturer's* recommendations

| Property | FM1000 | MasterBond EP-15ND |
|---|---|---|
| Typical Strength | 75–83 MPa (or 11–12 ksi) | > 83 MPa (or > 12 ksi) |
| Shelf Life | ∼ 6 months | ∼ 1 year |
| Recommended Curing Cycle | 60 min at 175 °C with 0.17 MPa pressure | 149 °C – 177 °C for 60 – 90 min |
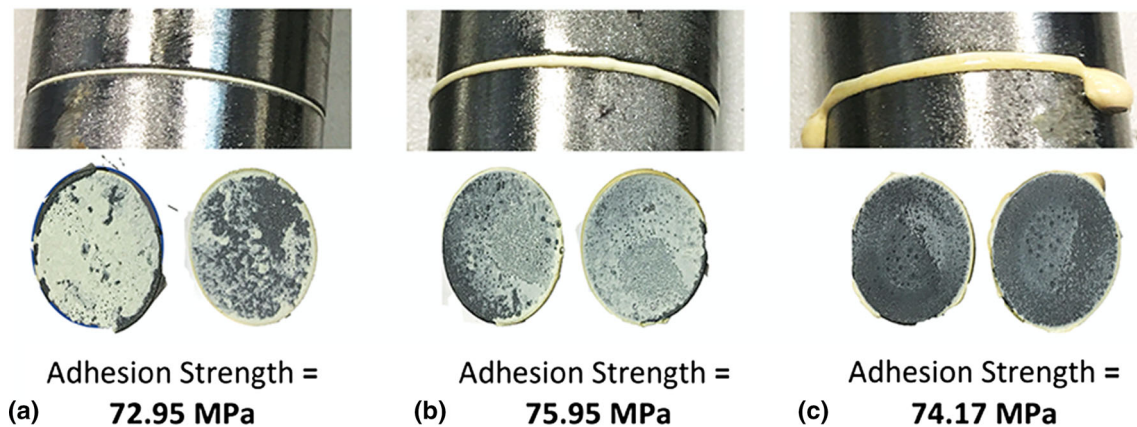


**Fig. 6** Spectrum of variations observed in the accumulated glue post-curing in three TAT glue samples and the pictures of the interface after failure. Irrespective of such glue residues, all the specimens still meet the expected strength requirement

increases. This effect can understandably be more pronounced when testing highly porous coatings, as capillary forces from interconnected porosity promote glue infiltration. This limits the reliability of TAT results of thin, porous coatings. Therefore, the ASTM C633 guideline recommends that the coating thickness be greater than 380 μm (Ref 35).

Other than glue infiltration, another consequence of viscosity loss is the spread and subsequent accumulation of an overflown glue residue along the sample periphery upon cool-down. Figure 6 shows in-house data of three TAT specimens that evaluated the glue strength of FM1000. The figure illustrates the extent of variation possible in such glue peripheral residues as shown in the photographs before and after TAT of three-rod substrates cured simultaneously in a gradient-free furnace. Reference Glue TAT specimens are simply two mating substrates glued together with no coating present, which are cured in the same heating cycle/batch to study the validity and reproducibility of the in-house curing approach.

Some sites prefer to grind off the glue residue before testing, while others do not. However, the results from the in-house experiments indicate that the strength of all the three specimens, with varying extents of peripheral glue residues, was within the acceptable range of the supplier's specification for FM1000. Consequentially, it can be concluded that the glue residues did not significantly affect the glue strength.

*Effect of Glue infiltration*

Although glue infiltration in the coatings is undesirable, it is not entirely avoidable, especially in the case of porous coatings due to the capillary infiltration forces. This phenomenon was investigated earlier by Wigren et al. (Ref 32), where the tensile strength of Ni–Al/alumina coatings was reported to vary between 15 and 60 MPa depending on the glue and curing method used. Figure 7 shows the data adapted from the work.

According to the accepted guidelines established in the bond strength testing of thermal spray coatings (Ref 56), coatings of thickness greater than 250 microns can be tested if the coating porosity is less than 2%. ASTM C633 standard, however, restricts testing of any coating thinner than 380 microns. In contrast, ISO 14916 explicitly recognizes infiltration as a fault source for thin coatings.

**Role of Testing Methods**

A set of in-house experiments investigated the variations in FM1000 adhesive strengths when equivalently cured onto a rod geometry TAT specimen to probe the significance of the testing methodologies. Four glued sets (with 5 samples in each set) were subjected to load-controlled tests (at 1kN/sec and 3 kN/sec) and position-controlled tests (13 μm/sec and 39 μm/sec). The results did not exhibit significant differences, as shown by the average glue strengths for the
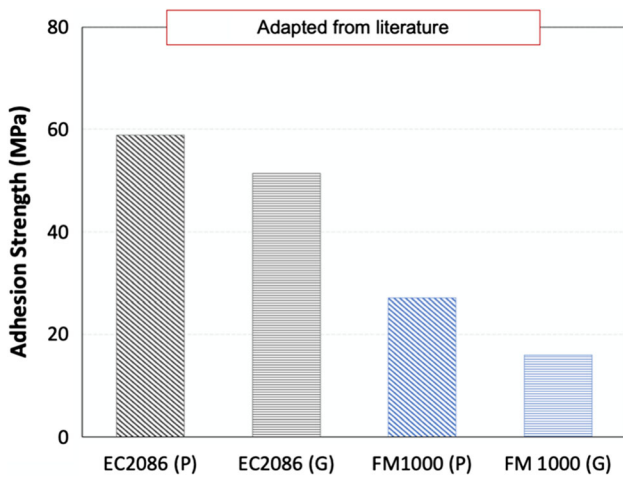
**Fig. 7** Results adapted from the work of Wigren et al. (Ref 32) highlighting the difference in adhesion strengths observed for a control NiAl/Al2O3 coating system when cured with four combinations of glue type (EC 2086 and FM1000) and curing process (Pressure (P) and gravity (G) assisted)
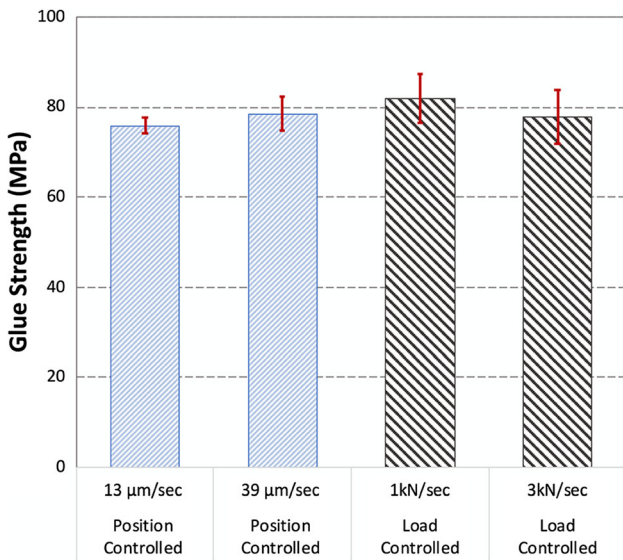


**Fig. 8** Comparison between glue strength observed with position and load-controlled tensile tests, highlighting that the values are not significantly different in the absence of coatings. The data shows five individual specimens' average glue strength and the standard deviation in the five measured strengths

four sets in Fig. 8, indicating that loading rate and method (position vs. load) does not significantly impact the test result.

## Variability in TATs

The variability in the TAT result is a qualitative descriptor of the variations found in the strength (critical load and plane of fracture) when the same test is repeated on an equivalent set of samples (same materials, process, deposition parameters, thickness, substrate geometry).

Variability in TAT results is a major drawback of the test. Such variability can arise from two mutually exclusive sources: the testing methodology (extrinsic source) and sample characteristics (intrinsic source). The previous subsections have addressed the role of the well-recognized extrinsic factors in the testing methodology that induce variability in strength measurements.

Intrinsic variability in TAT tests arises due to the incremental nature of thermal spray deposition. A typical thermal spray coating–substrate interface is a contact plane between multiple individually solidified splats and a continuous (bulk) substrate. The inter-splat boundaries and intra-splat features (i.e., microcracks) and any debonded areas (due to debris, pores, or spallation of splats) all give rise to what manifests as a reservoir of randomly distributed defects (or flaws) at the coating–substrate interface. The length scales and the individual character of such flaws (whether primarily globular pore, microcrack, or just a gap) cannot be quantitatively analyzed for each sample. Among such flaws, the ones partially or totally aligned along the interface with a sharp tip (i.e., a radius of curvature approaching zero) can act as failure initiation sites when subjected to tensile forces. As the distribution and density of such flaws (along the interface with a sharp tip) are impossible to quantify and control, TAT tests have an inevitable variability arising due to the differences in the flaw leading to interfacial failure.

A popular method to quantitatively characterize the statistical variability observed in the strength of brittle materials governed by "weakest-link failure phenomena" is the Weibull analysis (Ref 28, 52, 53, 57, 58). The Weibull distribution model maps the probability of failure at varying stresses with the help of two parameters: the characteristic strength and the Weibull modulus. Characteristic strength defines the magnitude of the stress where 63.2% of the population of samples fail. Weibull modulus is a quantitative measure of material strength distribution (or variability). A higher Weibull modulus implies a low variation from sample to sample, and a single strength value can be used to characterize the system. The physical significance of a high Weibull modulus in a system indicates uniformity in the distribution of flaws in the material. The following subsections assess the extrinsic and intrinsic variability from reliable industrially generated high-volume TAT data for multiple thermal spray systems with the help of Weibull analysis.

### Extrinsic Variability Induced via Testing Methods

Extrinsic variability of the TAT has been addressed in the past with 'round-robin' studies. In a typical round-robin

investigation, identically deposited samples are subjected to the unique site-dependent TAT testing methods. The pioneering round-robin work for understanding TAT extrinsic variability was done by Evans in 1992 (Ref 59) with participation from 19 independent labs on NiCrAlY coatings on Al cured with FM1000 and EC 2086/EC 2214 glue. The results (adapted in Fig. 9) reported ∼ 20% variability in the average measured adhesion strength from the various sites despite maintaining consistent sample geometry, materials, and properties. Another important finding from this study was that the scatter in the data collected from the FM1000 samples was lower than the other epoxy-based glue.

Another prominent contribution in assessing the extrinsic variability in TAT experiments associated with testing methodologies was published by Berndt (Ref 33). In this study, Weibull analysis was conducted on adhesion strength results of plasma sprayed alumina coatings obtained from three sites using four glue combinations (results adapted in Fig. 10). The investigation also reported a combined Weibull modulus for the measurements, which was generated by analyzing the extensive dataset created by combining data from all three sites.

It is evident from the strength data in Fig. 10 that each independent site had a different Weibull modulus of adhesion strength for equivalently deposited coatings. This emphasizes the issue in using TAT results for specification: interfaces with identical origin exhibiting distinct Weibull modulus and, therefore, different average strength (for instance, for set 2A from site A vs. site C). The results from these two literature studies illustrate how TAT results can

conclude differently for identically processed samples tested at different locations.

### Intrinsic Variability Induced via Specimen Characteristics

Hundreds of similarly fabricated samples should be tested to assess the microstructurally induced intrinsic variability in the TAT test. In Weibull analysis, the characteristic strength is strongly influenced by the sample (data) size; therefore, an extensive dataset assists in reducing the population-driven bias. Consistent testing methods are required to reduce the contribution from extrinsic factors as much as possible. Understandably, data conforming to these two conditions is hard to generate/acquire in an academic setting and was not found in the existing literature. Therefore, data contributed from industrial production sources was requested and compiled to present a discussion on the extent of variability in multiple thermal sprayed systems.

The industrial data was synthesized and evaluated via the Weibull methodologies, and the results are summarized in Table 3. Each data point input for the Weibull analysis was an average adhesion strength value obtained by testing three equivalently sprayed prepared samples. Table 3 also reports the relative percent of 100% adhesively failing sets of samples within a given system, indicating that the variability was observed in the magnitude of critical load and the fracture plane.

Often the TAT specimens of HVOF-sprayed carbides fail in the glue layer, and this is accepted as a conclusive result that suggests the interface is stronger than the glue strength. Since FM1000 is a polyamide polymeric substance (with some elastic–plastic regime), it does not undergo brittle fracture. Therefore, the high Weibull Modulus for HVOF WC–Co coatings and FM1000 glue shown in Table 3 is justified.

Another critical observation from Table 3 is the correlation between the fabrication process and the Weibull modulus. Industrially prepared HVOF coatings analyzed here universally show a higher Weibull modulus for their adhesion strength, and concurrently there is a higher percentage of conclusive adhesive failure tests. This is in reasonable agreement with the microstructural characteristic of the HVOF metallic and cermet coatings, which would have significantly fewer flaws than APS counterparts (due to the nature of splat formation and coating formation dynamics (Ref 60-62)). Further information on the intrinsic variability of the TAT tests can be extracted by analyzing the raw Weibull data.

Figure 11 highlights the Weibull analysis comparison for the HVOF and APS Tribaloy T-800 coatings on steel. The results have two characteristic features of importance: The magnitude of the modulus and the nature of the linear
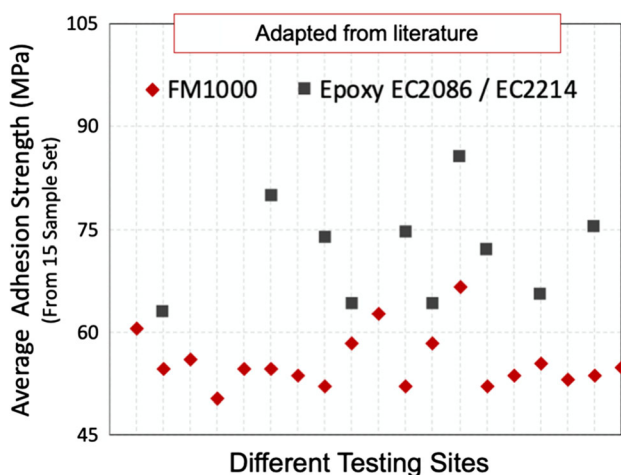


**Fig. 9** Results adapted from work by K A Evans (Ref 59) that presents the results from the round-robin study emphasizing the site/operator bias in adhesion strength results. Another takeaway from the result is that the FM1000 wafers exhibit a lower variability across sites than the epoxy-based counterpart

**Fig. 10** Adapted results from work by Berndt (Ref 33) that present the Weibull modulus for plasma-sprayed alumina coatings tested at three different sites with four variations of glue types and curing procedures
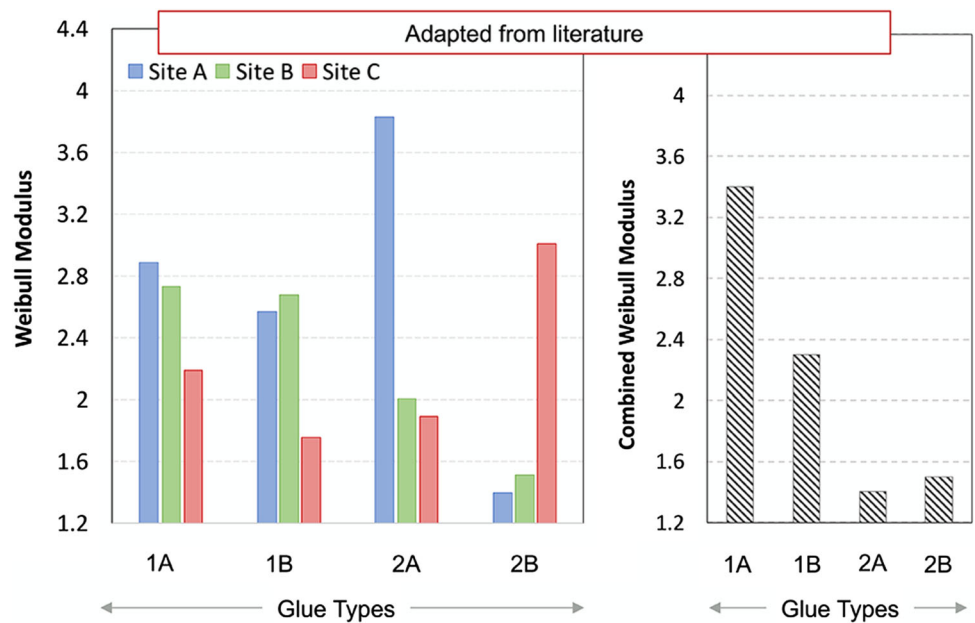


**Table 3** Agglomerated data collected from reliable industrial databases (equivalent coating-substrate systems, tested with consistent methods) highlighting the Weibull modulus and characteristic strengths of various thermal sprayed systems

| Material | Process | Weibull Modulus No unit | Characteristic Strength MPa | Mean Adhesion Strength MPa | Sample Size No unit | % Tests with 100% Adhesive Failure in population No unit |
|---|---|---|---|---|---|---|
| Aluminum Bronze | APS | 6 | 25 | 23 | 281 | 59 |
| T 400 | APS | 9 | 40 | 38 | 2233 | 54 |
| | HVOF | 18 | 66 | 65 | 1321 | 69 |
| T 800 | APS | 6 | 44 | 41 | 7723 | 48 |
| | HVOF | 16 | 71 | 69 | 2994 | 52 |
| CrC-NiCr | APS | 10 | 48 | 45 | 4254 | 61 |
| NiCrAlY | APS | 6 | 59 | 55 | 296 | 89 |
| WC–Co | APS | 11 | 62 | 59 | 785 | 63 |
| | HVOF | 21 | … | … | 1326 | Glue Failure |
| FM1000 Glue | … | 27 | … | 79 | 2488 | Glue Failure |

fit. From the figure, the HVOF T800 coatings exhibit a higher Weibull modulus and better fit (higher $R^2$ value) compared to the APS T800 coatings.

The lack of a good Weibull fit on a TAT dataset suggests an inconsistent or stochastic underlying flaw population, assuming the material was tested consistently and failed in a brittle manner. Conversely, a good Weibull fit is sometimes indicative of a single, dominant reproducible flaw type. Therefore, the Weibull analysis can be a powerful tool in describing the contribution of the microstructural features of thermally sprayed coatings and the flaw distributions on the intrinsic variability of the TAT results.

APS coating will have more pores and microcracks than the HVOF counterpart. From a fracture perspective, a round pore is typically considered a blunt flaw (with no sharp stress-concentrating tips). It is less likely to cause failure when subjected to external load than a sharp crack of the exact dimensions. However, it can still reduce the effective bonded region at the interface, assist in flaw propagation and even participate as a stress concentrator depending on the nature of defects in the vicinity. Thus, while testing thermally sprayed coatings, if some test specimens fail due to existing microcracks and others fail due to pores, the Weibull distributions of these specimens with different flaw populations will still overlap to some degree (i.e., APS T800, Fig. 11). In this scenario, it is
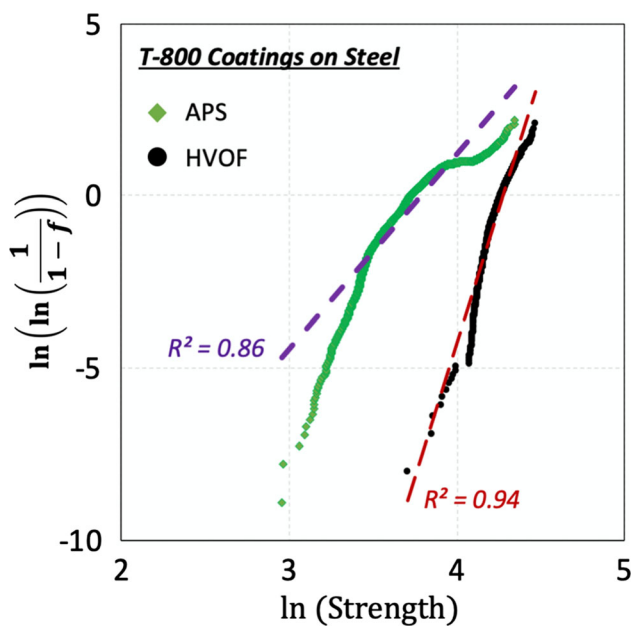
**Fig. 11** Comparison between the Weibull plots of Tribaloy T-800 coatings on steel fabricated via APS and HVOF processes. (Note that 'f' represents the probability of failure, calculated as $f = \left(\frac{\text{Rank} - 0.5}{\text{Total Count of samples}}\right)$)

impossible to isolate the source of intrinsic variability that led to the failure, and the Weibull strength distribution will not have a smooth continuous fit. If a substantial number of specimens are tested such that *two* distinct Weibull distributions are discernable, the failure results from multiple flaw types. The interface of HVOF coatings has fewer defects than APS coatings. That implies that the fracture in such HVOF coatings is dominated by a singular flaw type, which will yield a relatively better fitting Weibull data with a higher Weibull modulus.

This understanding of these two sources of variability and their contributions to the measured adhesion strength, when considered conjunctively with the fact that TAT results are used as a specification parameter for quality control (i.e., go/no-go), leads to two crucial questions. First, is it possible to decouple the extent of procedurally imposed variability from the data? Second, is the adhesion test a reliable quality indicator of consistency in deposition if the extent of intrinsic variability is not previously known/quantified?

## Interface Attributes in Tensile Adhesion Test

This section is presented in three subsections: Interface properties (roughness), Processing route (fabrication method), and Depositional Parameters (thickness and microstructures).

## Role of Interface Properties

### Interface Roughness

Several studies have reported that increased interface roughness (quantified with arithmetic roughness parameter $R_a$) positively impacts the adhesion strength. However, among the extensive pool of literature, results from some investigations reporting mixed-mode (or inconclusive) failures in TAT samples cannot be used in establishing property-adhesion trends (Ref 45, 47, 49, 63). It is incredibly challenging to determine the site for failure initiation in samples that show inconclusive fractures; therefore, the measured strength magnitude cannot be conclusively associated with the interface. For example, the investigation by Staia et al. (Ref 49) and Guilemany et al. (Ref 47) on High-Velocity Oxy-Fuel (HVOF) Tungsten Carbide (WC-Co) coatings on copper substrates observed an increasing strength with higher substrate roughness with two independent tests—Indentation and TAT (ASTM C633). However, the TAT results clearly show mixed-mode failure.

On the contrary, certain studies have reported inconsistent trends in adhesion strength with increasing roughness. Work by Hadad et al. (Ref 29) reported adhesion strength results obtained via the EN 582 test (Ref 64) for flame-sprayed alumina and Ni–Cr coatings on steel and TiAl6V4 substrates. The study suggested that the impact of interface roughness on adhesion strength was not directly evident. Khan et al. (Ref 63) analyzed an APS CoNiCrAlY/YSZ system on Hastelloy buttons. It was observed that on increasing the interface roughness (by varying how the bond coat is grit blasted after deposition to inherently change its surface roughness), the strength initially improved and declined on further roughening. This study also reported a switch from adhesive failure to mixed-mode failure as the bond coat roughness increased. Consequentially, despite the high volume of work in this area, an understanding of the governing principles of the mechanical anchorage mechanism as they correlate the interface roughness to the adhesion properties is limited.

Figure 12 compares the observed in-house data on the adhesion strength of equivalent APS YSZ coatings deposited on aluminum rod TAT substrates with different surface roughnesses. The surfaces were prepared by grit blasting with alumina of varying grit sizes (#24-grit and #16-grit) to acquire different surface roughness. Additionally, a specimen was sprayed with the TAT rod in the as-received condition (with no surface preparation other than degreasing by ultrasonication). A profilometer was used to measure the interface roughness on all the TAT substrates before deposition. The reported roughness measurements in µm are average $R_a$ values from 10 individual surface
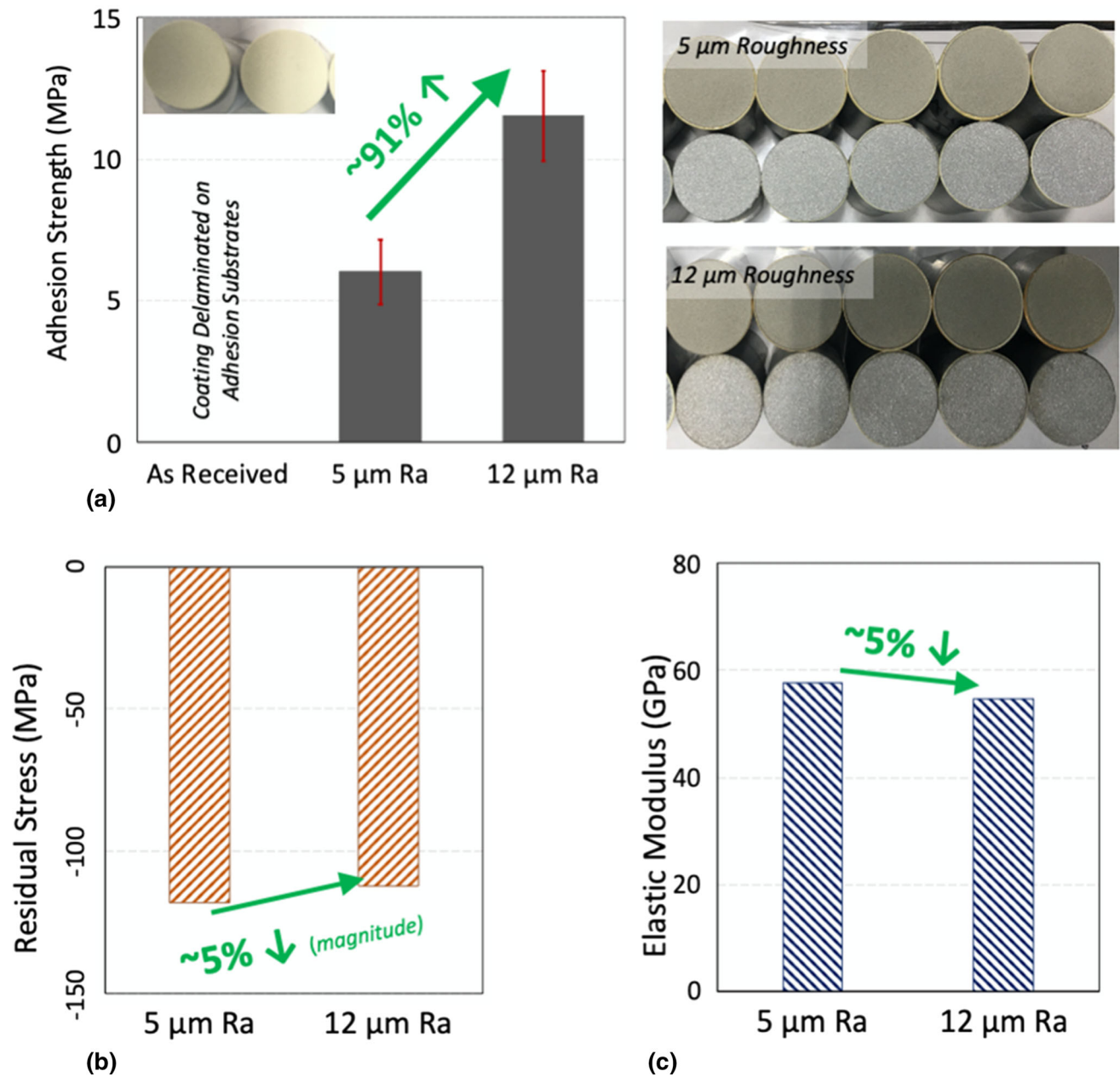
**Fig. 12** (a)Comparison among the adhesion strengths of three equivalent APS YSZ coatings deposited on aluminum 6061 substrates with different roughness along with the post-test pictures. (b) Residual stress and (c) Elastic modulus for these sets of samples were also measured via beam curvature measurements and had comparable values

roughness measurements using the profilometer. Elastic modulus and residual stress in the coating were also measured using beam curvature methods for bilayer samples deposited on equivalent rough substrates (Ref 65, 66).

For this systematic in-house study, all the specimens failed at the interface and had a clean adhesive failure. Note that in the reported pictures, there are two rows of samples. The top row is the mating substrate, and the bottom row is the coated substrate. The photos indicate that the coating delaminated at the interface and remained

attached to the mating substrate due to the glue. The coatings deposited on the as-received substrates (i.e., without grit blast) delaminated from the substrates soon after deposition, indicating poor adhesion.

The results from Fig. 12 report that upon increasing the substrate/interface roughness, the adhesion strength (as measured by pure adhesive failure) improved—thereby establishing a definite positive correlation for this set of investigated samples. However, among the quantified mechanical properties of the system, both the elastic

modulus and residual stresses of the coatings had comparable magnitudes (± 5%). Thus, the observed positive correlation cannot be justified only considering the differences in the mechanical properties of the system. One popular school of thoughts on this issue suggests that the roughness profile affects the bonding at the interface (Ref 67, 68) and provides different extents of resistance to propagating flaws. However, experimental validation for this hypothesis has not yet been reported in the literature.

## Material Properties

### Substrate Material

Substrate material influences three critical factors: elastic mismatch (associated with stress distribution at the interface), roughness profile (response to grit blasting), and the participating mechanisms (susceptibility to deformation and metallurgical bonding) (Ref 68, 69). To complement the existing literature data, systematic in-house data was generated to study the influence of substrate alloy on coating adhesion strength. Surfaces of 6.35 mm-thick disks from three substrates (aluminum, steel, and Inconel 718) were prepared to have similar surface roughness, $R_a$. The substrates were then coated simultaneously in one deposition run (to maintain a comparable deposition history on all samples) with porous APS YSZ coatings ($\sim$ 400 µm). The coated disks were assembled into a TAT disk geometry specimen and tested. Analogous samples on relatively thinner beam curvature substrates ($\sim$ 2.2 mm thickness) of the same substrate compositions were also fabricated to calculate the change in stress for different substrates. Although the stress states in the disks will not be exactly comparable to the stresses estimated via the beam curvature measurements, the values generated from these experiments still provide an insight into the relative trends that can be expected. In this set of experiments, the choice of APS YSZ as the coating material was deliberate to minimize the possibility of metallurgical bonding/interaction during deposition.

The observed results from the in-house tests are shown in Fig. 13. All the samples in this set of experiments failed
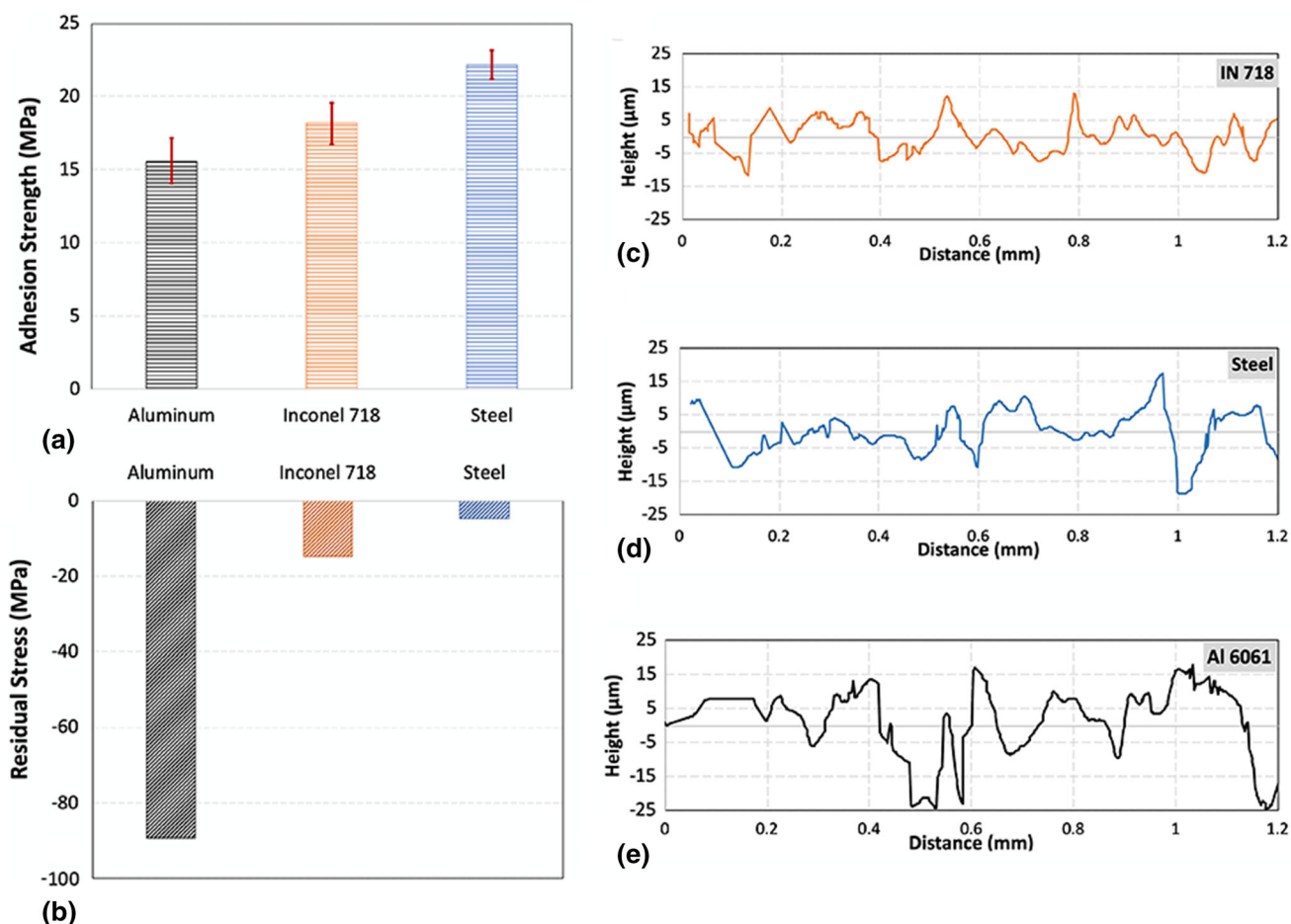


**Fig. 13** Comparison of the (a) adhesion strength, (b) residual stress, and surface roughness profile for three substrates- (c)aluminum, (d) Inconel, and (e) steel disks with roughness (Ra) of 7 mm deposited with APS YSZ coatings at equivalent deposition parameters

along the interface. Substrate material affected the adhesion responses for equivalently deposited coating. It should be noted that although the arithmetic parameter, $R_a$, for the surface roughness was controlled, the roughness character had qualitative differences (such as the peak-to-valley sharpness). These differences are addressed in the line profiles shown in Fig. 13(c, d and e) (Ref 69).

In addition, the beam curvature measurements reveal that the residual stress distributions in the samples were distinct. Discussion on contribution of the residual stress to adhesion strength is presented in Section "Coating Thickness". Thus, although it is agreeable to state that the substrate material affected the adhesion strength, it is challenging to decouple the individualized contributions (among the roughness, elastic mismatch, or residual stress) that led to the observed difference in adhesion.

### Coating Material

It is well established that thermally sprayed metallic coatings show higher adhesion strength than ceramic counterparts (for equivalent processing routes) (Ref 17, 70). It is argued that in the case of metallic coatings, the severity of the flaws (location, size, and sharpness) is relatively low. In addition, metallic coatings may exhibit some ductility, contributing to increased adhesion strength. In contrast, for brittle ceramic coatings, once there is sufficient energy to propagate a pre-existing flaw (i.e., microcrack), the delamination will occur almost instantaneously.

In-house experiments were conducted to compare the strengths of metallic vs. brittle coatings. For these experiments, $\sim 450$ μm of YSZ, Alumina, Ni, and Ni-5Al coatings were independently deposited on aluminum and steel TAT rods with equivalent deposition parameters via APS (Fig. 14).

The ceramic materials alumina and YSZ exhibited lower adhesion strengths than the metallic Ni and Ni-5Al coatings. The reason alumina shows lower strength compared to YSZ can be a testament to alumina's intrinsic lower fracture resistance (Ref 71). Few studies in the past by Cinca et al. (Ref 72, 73) and others (Ref 74, 75) have indicated that a thin alumina layer can be generated at the interface when Nickel-Aluminum coatings are deposited via thermal spray. Such thin alumina ligaments at the interface can provide preferential cracking sites susceptible to fracture. This can be the driver for the observed lower strength of Ni-5Al coatings as opposed to Ni in the presented results in Fig. 14. The most notable observation from the results of Fig. 14 was the cohesive failure of all the coatings when deposited on steel substrates as opposed to aluminum substrates. Failure images for Ni and Ni-5Al samples are reported in Fig. 14.

The effect of substrate geometry and material can be reiterated with the help of these observations again. Section 4.2.1 (Fig. 13) reported that YSZ/steel samples deposited with disk geometry failed adhesively at the interface. However, the equivalent coating investigated here with steel rod substrates failed inconclusively. In the YSZ/steel rod geometry TATs, one cannot comment if the interface was any stronger than the disc-substrate counterpart as the site of failure initiation in these samples is unknown. In contrast to steel substrates, YSZ/aluminum systems with equivalent coatings (same processing technology, deposition parameters, materials, and testing geometry) tested on both rod and disk substrates (Fig. 4, Sect. 3.1.1) failed 100% adhesively. Thus, it is emphasized that one cannot easily predict the potential failure modes and relative strength of equivalent coatings when any aspect of substrate properties is altered. Therefore, consistency in testing and methodology in TATs is essential.

### Coating Deposition Method

Different thermal spray processes can yield significantly different microstructures for the same coating material. The resulting variations in microstructural features also affect the system properties, including adhesion strength. This phenomenon is realized because changing the process affects both the particle impact energy and substrate temperature during deposition. The extent of plastic deformation induced on the substrate upon interaction with the particles throughout the deposition process can alter the interface's adhesive properties. Plasma-based techniques can yield high temperatures that enhance coating bonding via highly localized melting and/or deformation of the substrate. In contrast, particles sprayed by processes like HVOF can impinge the substrate at such high velocities resulting in plastic deformation even at relatively low substrate temperatures.

Luo et al. (Ref 76, 77) and collaborators (Ref 78) conducted an extensive study to compare the response of Ni and Ni-5Al coatings on steel TAT rod configurations using MasterBond as the gluing agent. The coatings were deposited via four distinct thermal spray processes: APS, TWA, HVOF, and CS. Results corresponding to fine roughness substrates are adapted in Fig. 15. It is evident from the reported results that the fabrication process for equivalent feedstock material can significantly affect the adhesion strength. In terms of coating chemistry, all the Ni–Al coatings from the investigated study exhibited relatively higher strengths than the Ni counterparts for all the processes. Supplementary elastic modulus and residual stress data for the equivalent samples of Ni coatings measured via beam curvature monitoring (Ref 65, 66) are also reported in Fig. 15. The data indicates a correlation
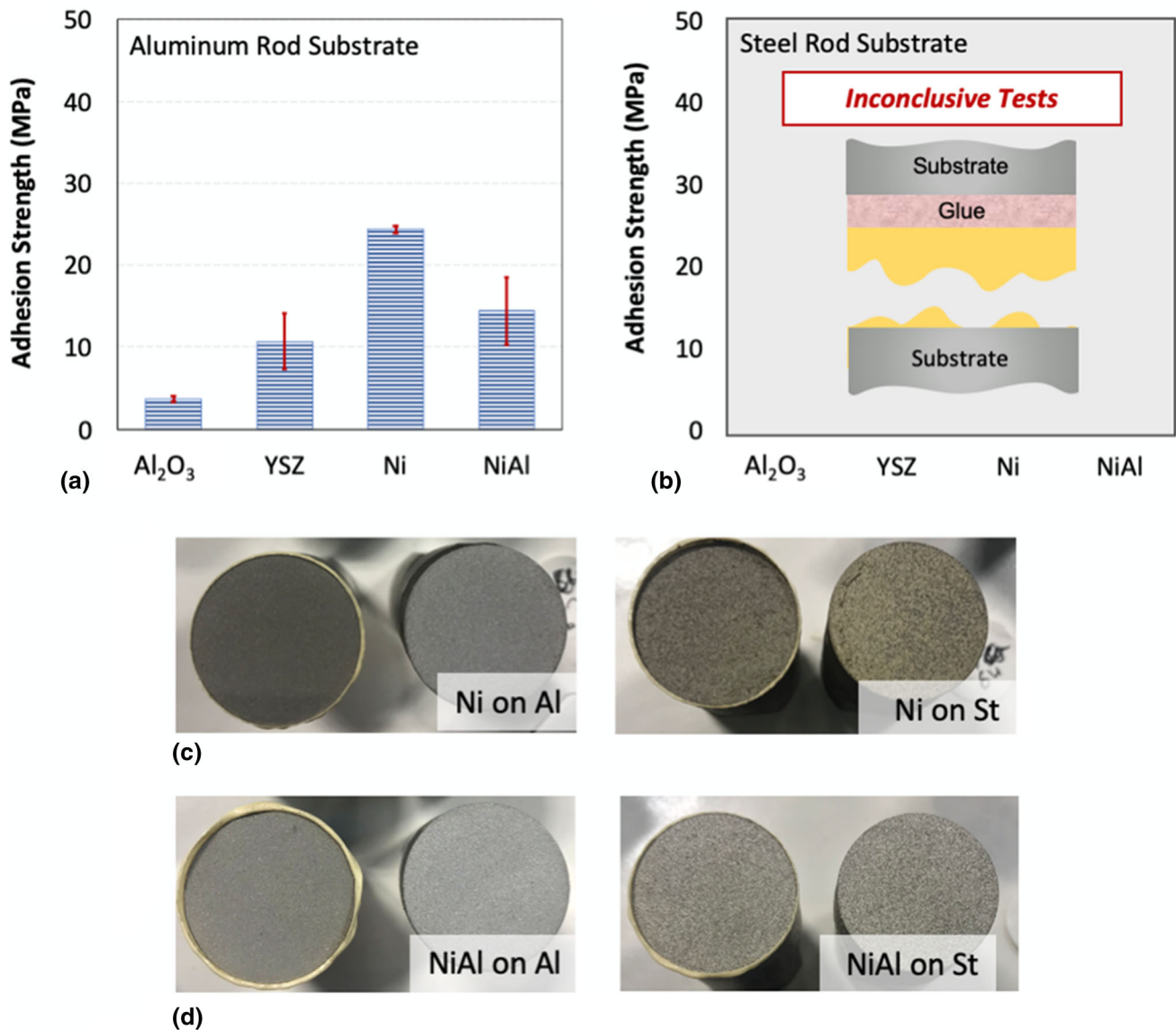
**Fig. 14** TAT results for multiple coatings (alumina, YSZ, Ni, and Ni-5Al) deposited with the same plasma parameters on (a) aluminum and (b) steel rod geometry substrates. The pictures at the bottom provide visual evidence for the adhesive mode of failure in the case of (c) Ni and (d) Ni-5Al on aluminum in contrast to the cohesive failure on steel

between the increasing coating modulus and adhesion strength. The residual stress also trends with observed adhesion strength; however, among the few available articles in the literature on the subject, a study by Greving et al. (Ref 79) explicitly suggests that the variations in residual stresses can contribute to changes in adhesion strength.

APS Ni/steel and Ni-5Al/steel systems were also tested in-house using aluminum and steel TAT rod specimens (reported earlier in Fig. 14) with FM1000 glue. In the in-house results, it was observed that the failure on aluminum was adhesive while the failure on steel was entirely cohesive. The contrast in results between systems of similar compositions reported in Fig. 14 and 15 emphasizes that

the adhesion test results are heavily influenced by the test methodology and coating parameters, which concurrently affect the actively participating bonding mechanisms. This observation also highlights the importance of specification when publishing TAT results, as arguments toward the adhesive properties of a coating/process are also highly dependent on the processing conditions.

The selected coating chemistries (Ni and Ni5Al) are convenient for comparing the interface strength between high and low-velocity processes. It is widely accepted that coatings deposited with sufficiently high particle velocity and/or impact energy by processes such as HVOF and Cold Spray usually have strong interfacial bonding due to high impact energies of the partially molten particles (Ref
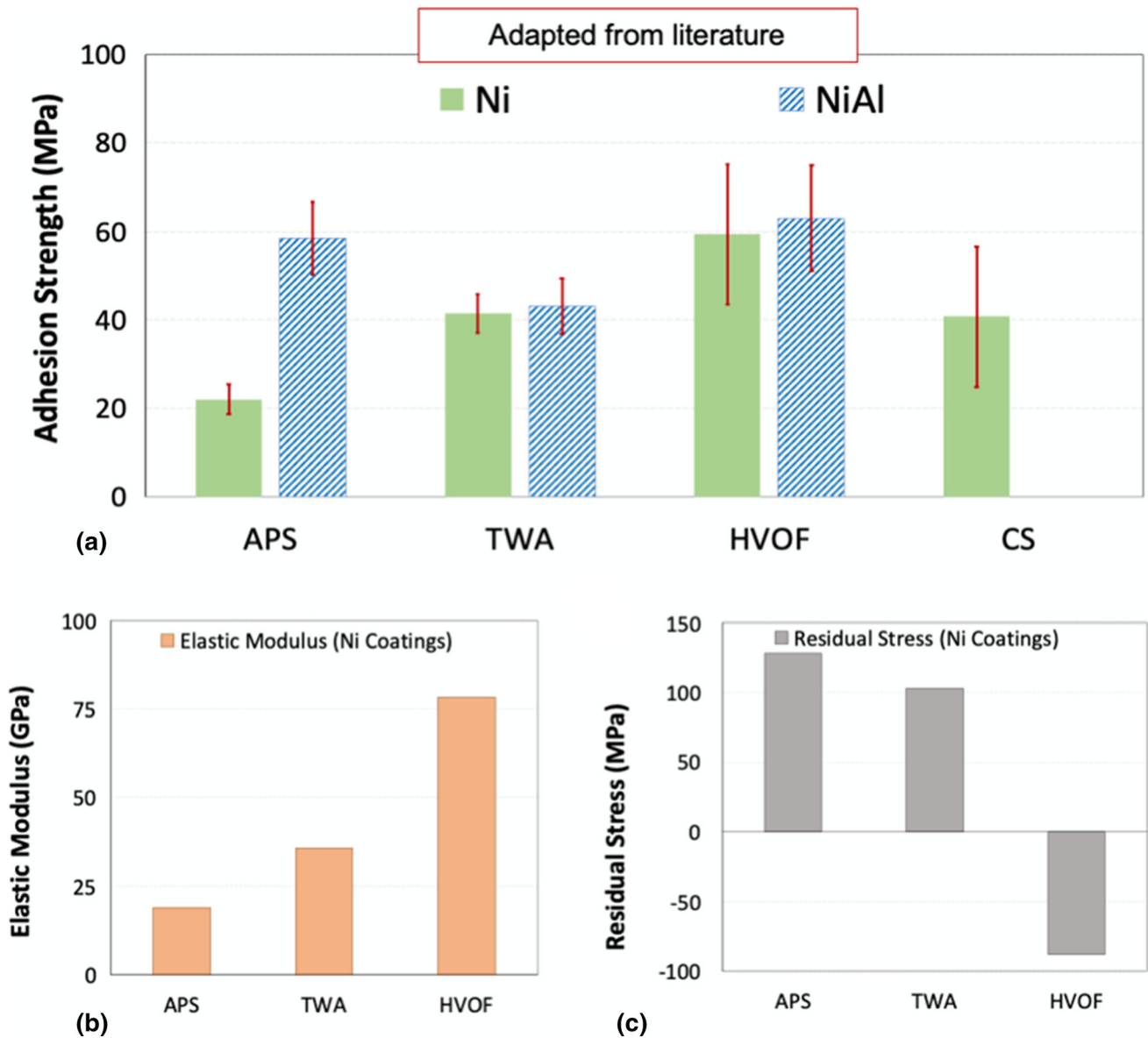
Fig. 15 Results adapted from the work of Luo et al. (Ref 76, 77) highlighting the dependence of the adhesion strength of Ni/Steel and Ni-5Al/steel systems fabricated via different processes. Additional available information for the (b) Elastic modulus and (c) residual stress of the equivalent Ni/steel coatings for some of the samples as reported by coauthors (Ref 78) elsewhere

80, 81). Therefore, the adhesive strengths in such samples typically exceed the maximum strength of glues such as FM1000, typically in the 69–76 MPa (equivalently 10–11 ksi) range. Thus, although a significant amount of data has been collected for such high-velocity deposition processes, very few of those results represent actual adhesive failures at the coating interface (i.e., not mixed-mode or glue failure). Therefore, the current understanding of the process-induced changes in the adhesion strength of HVOF and Cold sprayed systems is very limited.

To complement the work done by Luo et al. (Ref 76, 77) for metallic sprayed specimens, coatings were also deposited in-house via three analogous processes: APS,

Flame Spray, and Rokide™ Flame Spray on aluminum and steel rods. The results are shown in Fig. 16. The difference between Rokide™ and traditional flame spray is that the alumina feedstock in the Rokide™ process is introduced as a sintered rod instead of spherodized powder.

The pictures of tested samples in Fig. 16 provide an excellent representative example of inconclusive failures in the TAT test. In the case of flame-sprayed coatings on steel, only three of the five samples appear to have adhesive failure. Nevertheless, the cross-sectional microstructures revealed small fragments of adherent coating on the substrate. Moreover, the two samples that exhibited mixed-mode failure might have had an initiation site along the
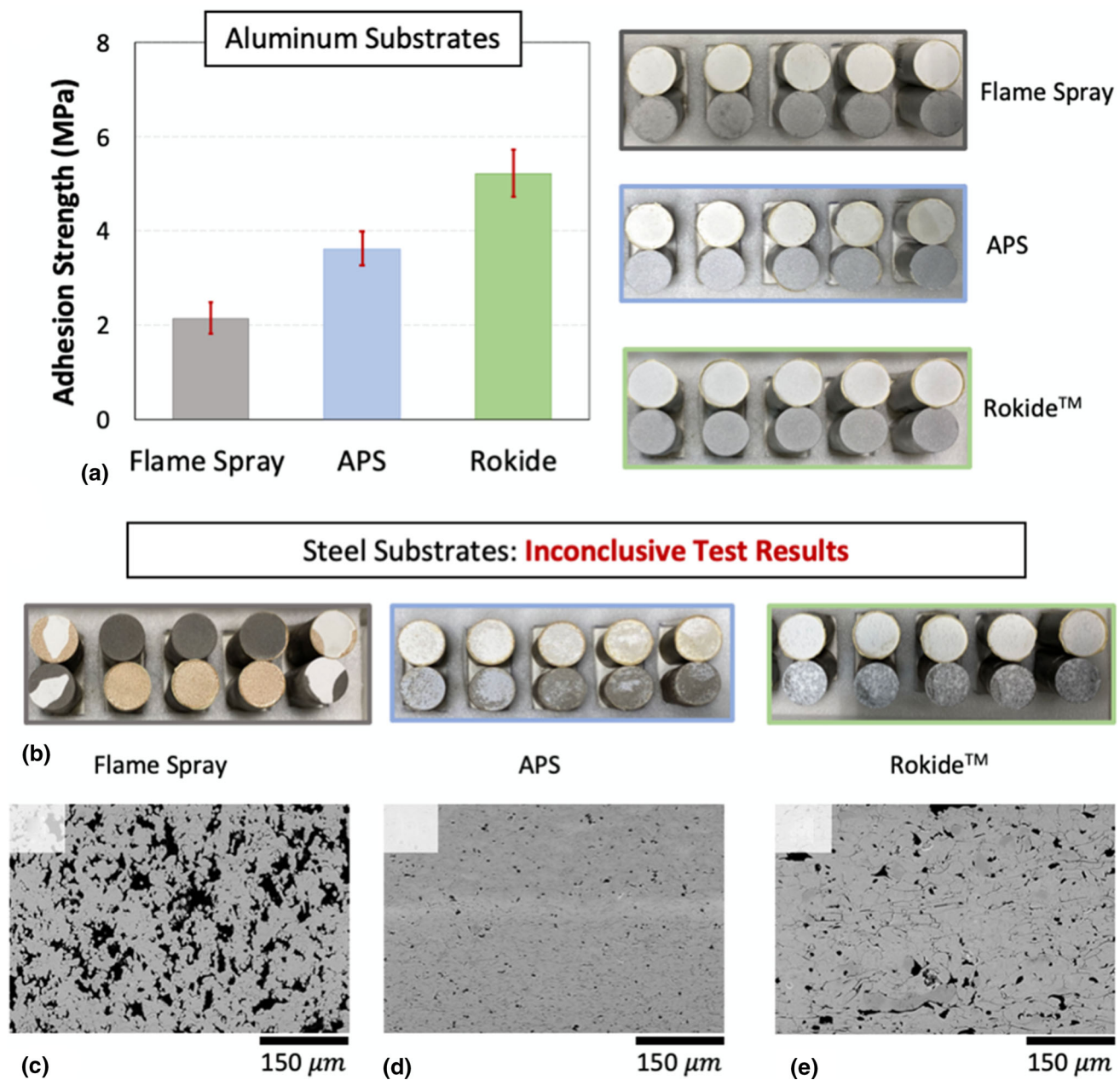
**Fig. 16** Variations in adhesion strength of alumina coatings incorporated due to the processing method on (a) aluminum and (b) steel rod geometry substrates with the photographs of the fractured specimen after TAT. Microstructures of the alumina coatings were deposited via (c) Flame Spray, (d) APS, and (e) RokideTM

interface, which propagated via the coating. Therefore, the results fail to reflect the adhesive characteristic of the system. The coating residue from the APS and the Flame spray coatings are more evidently visible on the steel samples and thus were also considered inconclusive tests.

All samples failed adhesively on aluminum substrates. The results indicate that the flame-sprayed coatings had the weakest interface. This result can be attributed to the microstructure, which indicates a low bonded area owing to the excessive number of voids and pores. However, among

the Rokide[TM] and APS alumina coating on aluminum, it is difficult to justify why a higher adhesion strength was observed for Rokide[TM]-sprayed coatings only using microstructural evidence and warrants further study that is outside the scope of this review.

## Role of Coating Thickness and Process Parameters

Deposition parameters can influence the bonding characteristics at the interface by contributing to differences in

interface temperature during coating build-up, coating thickness, and microstructure. High-temperature depositions (either by altering plasma parameters or externally pre-heating the substrate) can assist interfacial adhesion (Ref 85-87) by improving splat bonding. Moreover, higher temperatures can also render the substrates more susceptible to plastic deformation upon particle impact. All such factors can improve the interface adhesion (Ref 82-84). The following subsections highlight the influence of coating thickness and processing conditions on the adhesion strength.

### Coating Thickness

Several studies have reported that coatings of higher thickness tend to exhibit relatively lower durability, which is associated with a lower coating adhesion strength (Ref 85-88). The governing mechanism for such thickness-driven observations is known as the "free-edge effect," which describes the interaction of the residual stresses with overall coating thickness to contribute to a reduced adhesion strength (Ref 79). The free-edge effect is based on the stress distribution profile perpendicular to the coating plane, such that the system is in tension at the edge and in compression away from the edge. It suggests that coatings with higher thickness will have a higher propensity for interfacial debonding.

It should be noted that although coating thickness plays a role in the residual stress distribution at the interface, the magnitude of the residual stress is heavily affected by the processing methods and the parameters. And therefore, decoupling the correlations between the sample processing routes and properties with the residual stress is extremely challenging. This implies that determining influence of residual stresses on the bonding mechanisms that dictate the interface strength cannot be parametrically quantified.

Work by Greving et al. (Ref 79) provided accounts of wire-arc-sprayed Ni–Al coatings tested with the ASTM C633 standards for four coating thicknesses (adapted results are shown in Fig. 17). It was reported that adhesion strength decreased with increasing coating thickness. Likewise, other independent studies have also reported a decrease in the adhesion strength when the coating thickness increases (Ref 43, 44). However, based on the finite element simulations conducted by Greving et al., if the coatings were free of residual stresses, the adhesion strength would be independent of the coating thickness. Thus the study by Greving et al. (Ref 79) explicitly outlined that the residual stress distribution (not the coating thickness) is the critical factor affecting the coating adhesion strength.
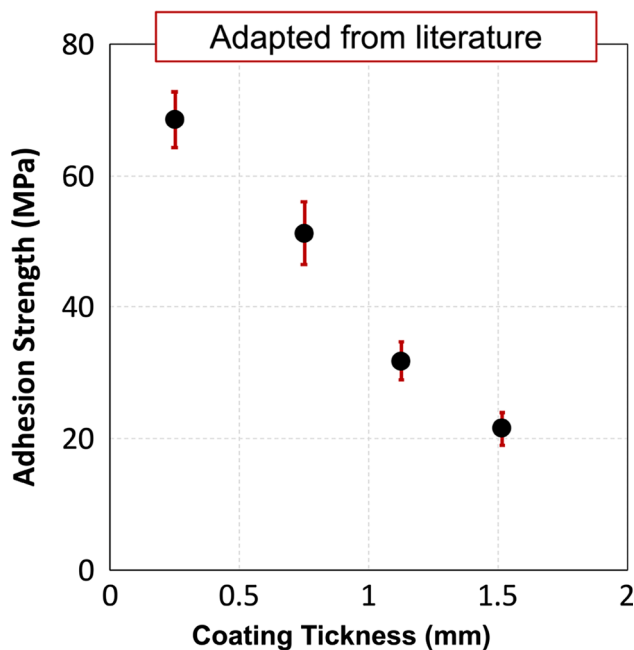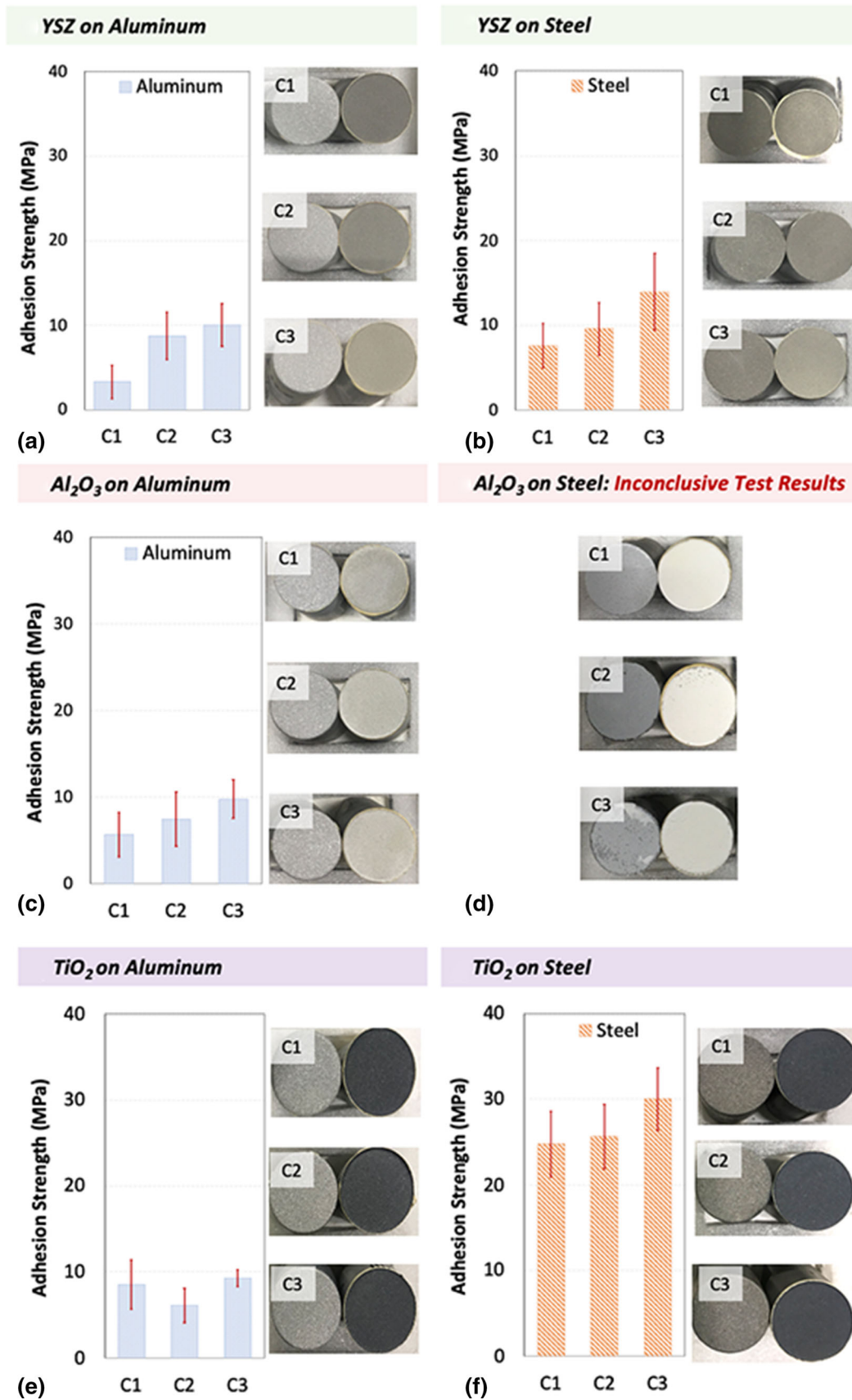


**Fig. 17** Effect of coating thickness on the average adhesion strength reported by Greving et al. (Ref 79) for wire-arc-sprayed nickel-aluminum systems deposited on steel

### Processing Conditions

Processing conditions can significantly alter the coating microstructure, which provides the most direct representation of the distribution of flaws in a coating, and therefore plays the most crucial role in determining the adhesion strength (Ref 61).

Figure 18 and 19 highlight in-house data that probes the effect of processing conditions on the adhesion test results. For the experiments conducted to compile the results for Fig. 18, responses of YSZ, alumina, and titania coatings were investigated on two TAT rod substrate materials: aluminum and steel. The coatings were deposited at three spray distances, 120 mm, 100 mm, and 80 mm and are labeled as C1, C2, and C3, respectively, in Fig. 18. (Further details in Appendix A.2).

The results from these in-house experiments on aluminum indicate that coatings sprayed at closer standoff distances always exhibited higher adhesion strength in all coating-substrate combinations. This is justified as at lower spray distances, the coating microstructures tend to have a lower flaw population, potentially due to stronger inter-splat bonding assisted with relatively higher deposition temperatures. YSZ and titania coatings failed adhesively on steel and were observed to have relatively higher adhesion strength than on aluminum. However, alumina coatings on steel had a mixed-mode failure, thus yielding inconclusive results.

(a) YSZ on Aluminum



(b) YSZ on Steel



(c) Al$_2$O$_3$ on Aluminum



(d) Al$_2$O$_3$ on Steel: Inconclusive Test Results



(e) TiO$_2$ on Aluminum



(f) TiO$_2$ on Steel

It is challenging to isolate what contributed to a stronger interface in alumina coatings when deposited on steel. Another interesting result is the relatively high magnitude of the titania coatings on steel substrates compared to the other ceramic materials. The underlying drivers that impart such high strength to titania coatings on steel are unclear, but the results indicate that the coating material affects the adhesive properties. Moreover, the YSZ/steel samples highlight the effect of processing conditions as the results from Sect. 4.2.2 (deposited via APS but with different torch and processing conditions) had an inconclusive failure in contrast to the samples reported in Fig. 18.

The details of the APS YSZ Samples in Fig. 19 are reported in Appendix A1, which were deposited using an F4-HB 90 plasma torch on aluminum and steel TAT rod substrates. The experiments here were centered around spray distance variations. Four spray distances were tested: 150 mm, 120 mm, 100 mm, and 60 mm (Labeled as P1, P2, P3, and P4, respectively, in Fig. 19). Specimen sets P1, P2, and P3 had a porous coating microstructure on aluminum and steel. Coatings deposited with parameter P4 had a segmented (or equivalently Dense Vertically Cracked, DVC) microstructure. The elastic moduli of these coatings are available in the literature (Ref 65, 66, 89).

The most noteworthy observation from this set of experiments was that none of the YSZ/steel samples had an adhesive failure, in contrast to the coatings obtained via a similar thermal spray process but a different operational torch (Fig. 18). Among the adhesively failing YSZ/aluminum systems, the DVC (segmented) coating interface exhibited a significantly lower strength than all the porous counterparts. This can be attributed to the microstructural difference in the coatings (Ref 65, 66).

## Discussion

In the prior sections, the key attributes of the TAT tests have been assessed through a critical analysis of the operating variables—both from the perspective of testing methods and processing nuances. Combining the available literature data with the appropriate insertion of in-house measurements to clarify phenomenological observations has identified key parametric contributors to the measured adhesion strength of thermally sprayed systems.

Results from previous sections highlight:

- TAT testing geometry can significantly affect measured adhesion strength. The in-house experiments showed that disc-geometry reports significantly higher adhesion strength than rod geometry. However, reused or chamfered substrates yield comparable strengths with respect to new and sharp-edge substrates.
- Variability in TAT results is a significant drawback of the test. The variability in the test results is inevitable, and it arises from differences in testing methodology as well as the nature and distribution of flaws at the interface. Statistical analysis like the Weibull method is necessary to develop a reliable understanding of the adhesive properties in a system.
- The coating fabrication process and deposition parameters play a crucial role in determining the nature and density of the flaws incorporated in the system and thus also affect the adhesion strength. The coating fabrication process partially determines which bonding mechanisms will participate at the interface. Therefore, similar coating-substrate combinations can yield significantly varying adhesion strengths when the processing route or deposition parameters are altered.

The following discussion attempts to integrate the results from previous results with a unifying theory based on fracture mechanics and bonding mechanisms.

## Variability and Uncertainties in TAT of Thermally Sprayed Samples

A few consistent empirical trends were observed in this article for the adhesion strength of thermal sprayed coatings. For instance, among the various coatings studied in this article that were deposited via APS, metallic coatings tend to yield a higher adhesion strength than ceramics. Another common trend that emerged from the results reported in Fig. 15, 16, 18, and 19 is the positive correlation between the elastic modulus of the coating and its adhesion strength. From the microstructural perspective, a coating with higher stiffness will have fewer flaws. Without a high flaw population, the critical stress to propagate delamination along the interface would have to increase significantly. Likewise, fundamental fracture mechanics principles dictate that the effective modulus of the interface ($E_{int}$) will increase with increasing coating modulus for a fixed substrate (Ref 90) since:

$$\frac{2}{E_{int}} = \frac{1}{E_{coating}} + \frac{1}{E_{substrate}} \tag{Eq 2}$$

Thus, it can be surmised that for reliably measured tests, the interplay between load distribution at the specimen interface, processing route, coating microstructure, and coating properties will all concurrently influence the
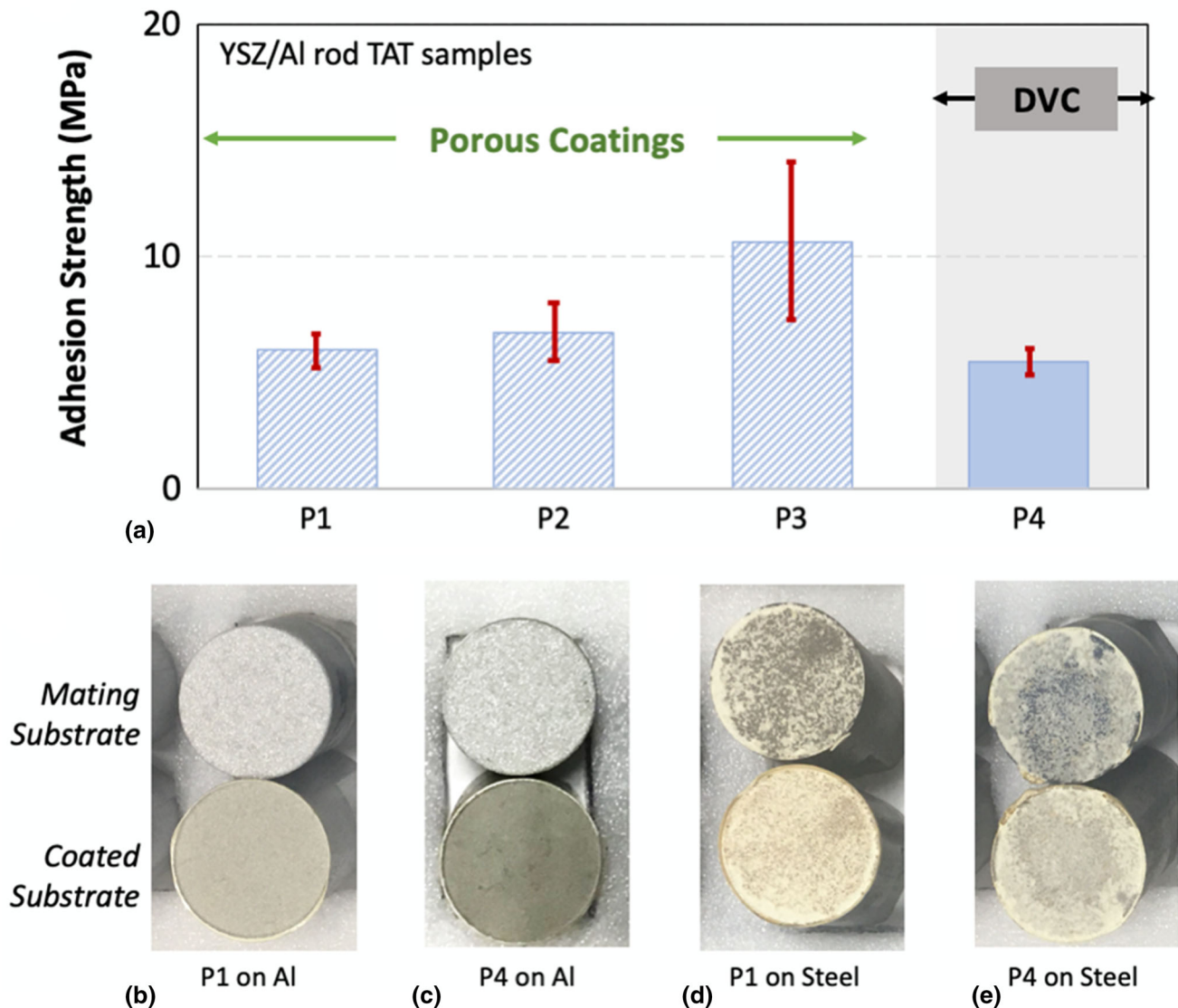
**Fig. 19** (a)Adhesion strength of YSZ coatings on Aluminum rod substrates. All the coatings failed adhesively on aluminum, whereas all exhibited inconclusive failure on steel. Failed specimens from representative samples are shown for (b) P1 on aluminum, (c) P4 on aluminum, (d) P1 on steel, and (e) P4 on steel, respectively

adhesion strength of the interface. This suggests that *the variability in the TAT results stems from the size, arrangement, location, and density of flaws present near the interface within the coatings.*

Each thermal spray process route (APS, HVOF, etc.) renders a unique collection of flaws and defects within the coating near the interface. Those flaws can affect the load-bearing area of the interface and can act as sites of stress amplification when subjected to external loads during TAT. Furthermore, equivalent coatings (same processing technology, deposition parameters, materials, and testing geometry) will still have a different distribution of characteristic flaws. In essence, the flaw distribution and flaw population cannot be precisely controlled from sample to sample. This variability in the flaw population and the non-uniformity of local stress distributions due to these flaws together contribute to the observed intrinsic variability in the adhesion strength measurements. Figure 20 attempts to schematically capture the various sources of variability arising between equivalently deposited samples from the intrinsic and extrinsic factors identified in previous sections.

Classical fracture mechanics expresses this relationship between the strength of a material/system, $\sigma$ (i.e., the critical load), critical stress intensity factor, $K_{IC}$ (resistance to cracking), and the critical flaw size, $a$, for a system that exhibits only Mode I fracture as:
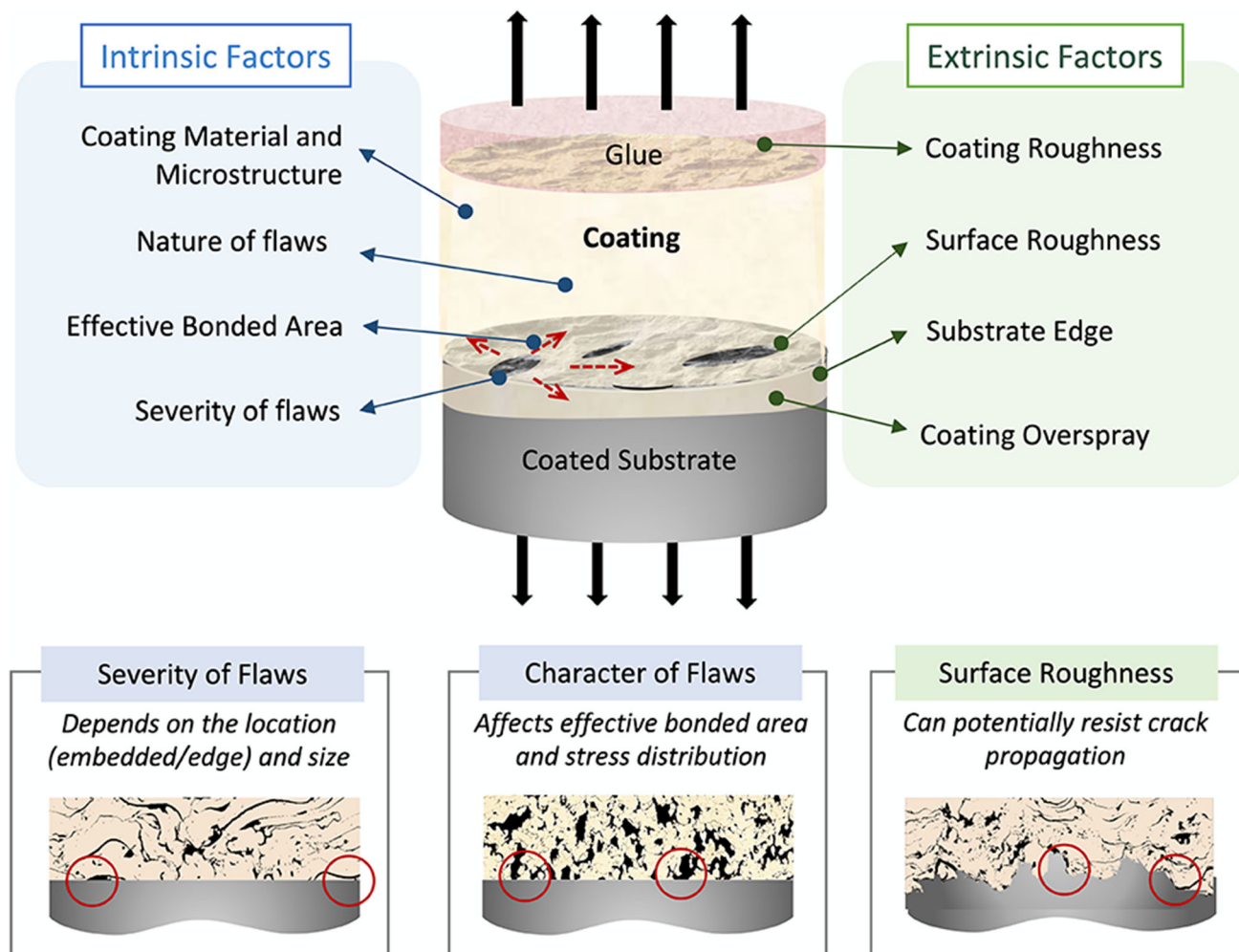
**Fig. 20** An illustrative attempt to showcase the intrinsic and extrinsic factors in a typical sample of a TAT set (equivalent samples deposited simultaneously) that can affect the observed load at failure in the test, thus imposing variability in the measured adhesion strength

$$K_{IC} \propto \sigma\sqrt{a} \tag{Eq 3}$$

It is important to note that Eq 3 is represented in its most simplistic form, ignoring the geometric factors related to the system's geometrical designs and dimensions. Equation 3 directly highlights the interrelationship of TAT results (that is, the quantitative measurement of the strength of a coating, $\sigma$) with a material parameter of the coating-substrate interface, $K_{IC}$. Thus, this can also be used as an indirect method to describe the repeatability/consistency in coating production sites (correlated to the similarity in the incorporated severe flaw, $a$).

When considering a TAT for quality control purposes, there is an indirect assumption that equivalently deposited coatings, when assembled carefully, should possess such a similar flaw population that the most severe flaw is comparable in size ($a$) from specimen to specimen. In an ideal scenario, when such a flaw criterion is met, the observed

TAT adhesion strengths between batches of specimens should be somewhat similar. This is what leads to the consideration of TAT data for quality control.

Likewise, consider a case of two distinct sets of coatings sprayed using different materials. If these two sets of coatings have similar flaw distributions, Eq 3 suggests the adhesion strength of the two sets should trend proportionally with the material fracture strength, $K_{IC}$, at the coating-substrate interface. Therefore, it is also plausible to consider TAT experiments as an indirect measurement of coating performance capability under simulative loads.

**Possible Pathways to Mitigate the Variability in TATs**

Minimizing the variability in TATs can be achieved by adopting practices focused on test fidelity and mitigating variations induced in the flaw population. However, as

stated in previous sections, acquiring a comparable flaw population in two sets of coatings is challenging to achieve and assess.

Several studies have proposed modifications to the adhesion test to partially circumvent this challenge in mitigating the variability in adhesion testing due to the variability in the population. For instance, the idea of introducing controlled flaws in adhesion specimens prior to TAT has been considered. In doing so, the coating failure initiation site is predetermined, and the flaw size is also known. With a controlled, predetermined flaw of a specific size, the fracture mechanics expressions can be numerically solved to extract the interfacial toughness. This approach has been demonstrated to a degree of success in the case of TBC ceramics by Qian et al. (Ref 91) and Okijama et al. (Ref 92, 93).

While adapting the TAT into a fracture toughness-driven test is an attractive concept, there are limiting factors for large-scale acceptance. As in other fracture toughness test methods, introducing a pre-existing flaw before/after deposition requires the flaw to act as a point of singularity for the fracture initiation. This means the flaw must behave as a sharp crack tip. As of this review, there is no methodology available that is unanimously accepted and considered convenient among the community which outlines how to introduce a sharp pre-flaw. Nevertheless, there are advantages to improving this approach—as it would not only allow for minimization of variability induced by the flaw population but also offers a method to measure the interfacial toughness of a thermally sprayed coating.

## Relevance of Interfacial Bonding Mechanism

The mechanisms that define the adhesion strength at the interface can be broadly classified as mechanical anchorage, metallurgical interaction, or plastic deformation (Ref 17). The individual extent to which these three mechanisms contribute to the overall measured adhesion strength depends on several factors. Some recognized contributors are the material thermophysical properties that define the system, the mutual as well as environmental or chemical reactivity between coating and substrate material at the deposition temperatures, and the energy of the incoming splats as they impact the substrate and build a coating. In general, the deposition temperatures and impact energies are governed predominantly by the nature of the fabrication process.

The magnitude of mechanical anchorage heavily depends on the interface characteristics before deposition, such as the substrate surface roughness, presence of contaminants, and the mutual affinity (i.e., the wetting angle of the incoming molten splats) between coating and substrate materials. It is possible to increase the contribution of mechanical anchorage to the adhesion strength by fine-tuning any interface characteristics, including roughness profile, substrate heating, in-situ laser cleaning, and operating in inert atmospheres.

Metallurgical bonding is known to be highly subjective to the materials that are forming or depositing at the interface. Metallurgical bonding is driven by the chemical interactions between the coating, substrate, and surrounding environment at the deposition temperatures (i.e., oxygen content, presence of inert gases or hydrogen, etc.). Unlike mechanical anchorage, process-controlled parameters like deposition temperature and impact velocity can affect the quality of metallurgical bonding. For instance, if the impact of the incoming particle breaches the pre-existing oxide scale on the substrate, it can potentially establish contact for metallurgical bonding, which can be further assisted by higher temperatures. However, in cases where oxides/brittle phases are generated at the interface, samples can exhibit lower adhesion strength by failing in the brittle layer.

Lastly, the extent of plastic deformation incorporated into the substrate during the fabrication of thermal spray coatings is determined by the impact energy of the incoming splat and the presence of (if any) localized thermal gradients. High-velocity processes (HVOF, cold spray) often induce localized plastic deformation at the site of particle impact. Such deformations may induce sufficient strains in the system to facilitate metallurgical bonding (for instance, by promoting bonding by breaking the pre-existing oxide scales on substrates) and thus, in turn, promote adhesion.

Figure 21 attempts to schematically capture these mechanisms in the context of measured adhesion strength. The figure seeks an association between the three generally accepted adhesion mechanisms with the data assimilated in this article from in-house experiments and data extracted from the literature (Ref 46, 80, 94-105). As noted earlier, higher adhesion strengths are noted for systems with lower defects accompanied by metallurgical interactions or plastic deformations. The process parameters that have the most influence are the particle thermal state and kinetic state. Well melted, high-velocity particles generally provide denser coatings and, in principle, should offer higher adhesion strength. A *new empirical approach* is presented here to depict the measured particle states as a summation of thermal and kinetic contributions to capture these two attributes. The idea is that these parameters can be collectively additive.

The thermal state of an incoming particle depends on the feedstock material's intrinsic properties (specific heat, the latent heat of fusion, etc.) as well as the mass of the impinging droplet. In the case of cermets, non-homogeneous melting is possible through the melting of the matrix,
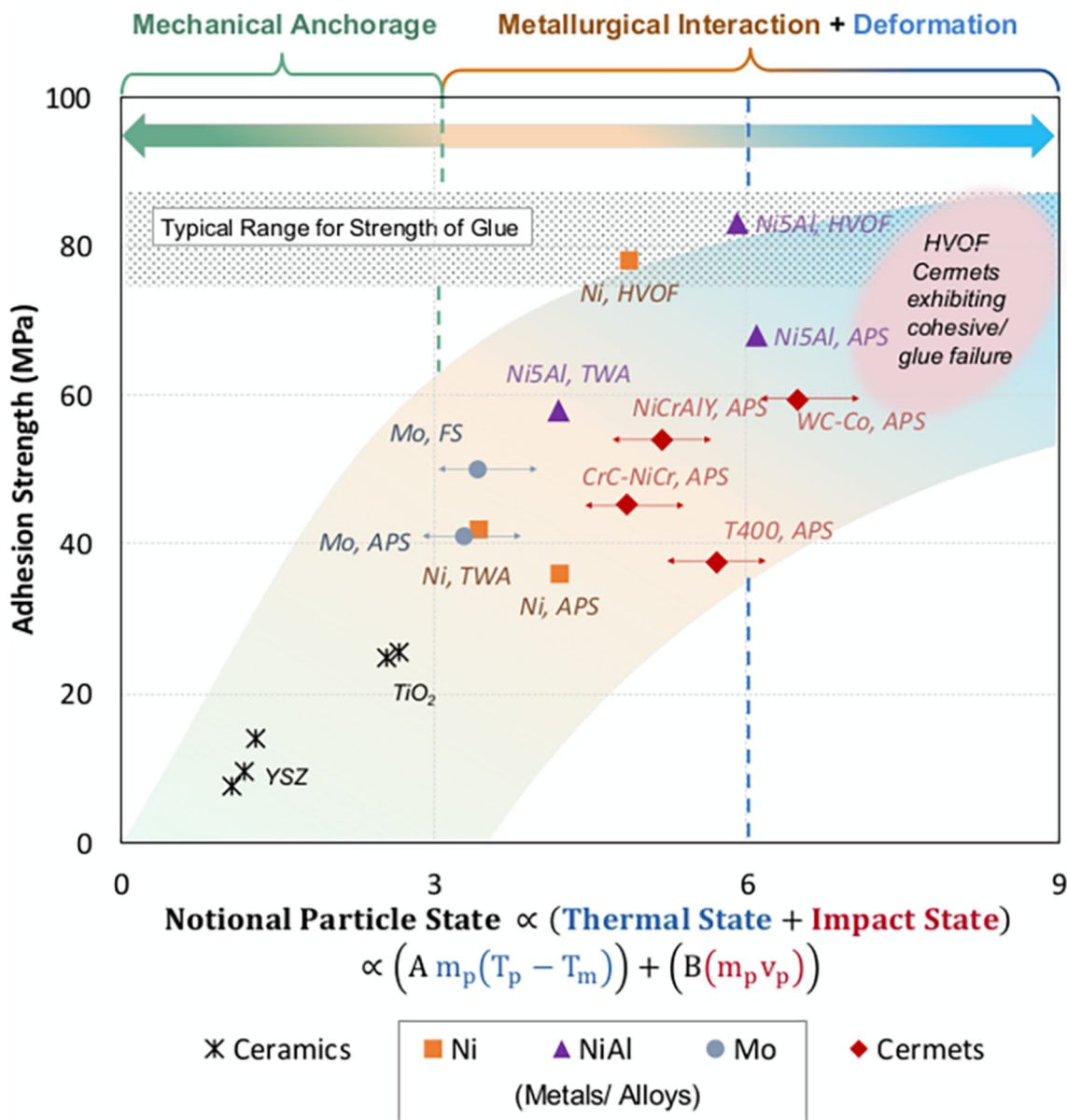
**Fig. 21** Notional (thermal + kinetic state) illustration of the role of interfacial bonding mechanism on the adhesion strength of various materials deposited by different commercially available thermal spray processes. The interfacial bonding mechanism is subdivided into three categories: mechanical anchorage, metallurgical interaction, and plastic deformation

while the hard phase does not undergo a phase transformation. Nevertheless, the hard phase provides substantial mass, which can contribute to the kinetic state through particle momentum. From these assumptions, the particle thermal state can be described as follows, i.e.,

$$Particle\ Thermal\ State \propto m_p(T_p - T_m) \qquad (Eq\ 4)$$

where $m_p$ and $T_p$ represent the mass and temperature of the particle that undergoes melting respectively, and $T_m$ is the melting temperature of the particle. This is unarguably a very minimalistic formulation, which fails to account for

the contributions of the latent heats, oxidation reactions, and the role of specific heat constants in estimating the thermal energy from the impacting particle. However, considering the vast scope of materials and processes to be encompassed in a unified qualitative approach, this preliminary formulation can provide useful insights that can be built upon in the future.

Note that in the case of low-temperature deposition processes like cold spray and HVOF, it is likely that the particle does not melt completely (or at all)—implying the thermal state will have a negligible contribution.

Meanwhile, the energy of impact of the incoming particle can be correlated to the extent of deformation that is sustained by the system. This can be expressed as proportional to the momentum of the incoming particle. Thus,

Particle Impact State $\propto m v_p$           (Eq 5)

where $v_p$ is the in-flight velocity of the particle, and $m$ is the mass of the impacting particle. This contribution will be much higher in high-velocity processes than other thermal spray processes. Since both thermal and kinetic states contribute to adhesion, a simple arithmetic sum of these two factors should provide a directionality to relate the participating adhesion mechanisms and, therefore, to adhesion strength. Note that it is still only possible to arithmetically combine these two terms after incorporating necessary coefficients to match the dimensions of the parameters (A and B, respectively), with magnitudes assumed to be 1. A preliminary framework of such an empirical correlation is presented in Fig. 21 (and associated data for particle temperature, velocity, and adhesion strength shown is taken from the references (Ref 46, 80, 94-105). Particle mass in for calculations are computed assuming a constant volume for all particles, and thus are proportional to the material densities ($\rho$). For stoichiometric compounds, like Al2O3, the density of the material was obtained from the literature. In the case of non-stoichiometric alloys and/or mixtures, for example, Ni5Al, the material density was calculated based on the volumetric contributions of the constituent elements (i.e., $\sum_i \rho_i V_i$ ).

While exploratory and empirical in nature, Fig. 21 captures the anticipated effects of processing and material variables on the adhesion strengths. The figure further identifies possible operating mechanisms that govern the relevant adhesion strength numbers. Specifically, the figure highlights the typical ranges of adhesion observed among the most common archetypes of coatings (ceramics, alloys, and cermets) and processes (flame spray, plasma, HVOF). For instance, Fig. 21 shows the adhesion strength of thermally sprayed oxides to be generally lower than metals and cermets irrespective of the processing route. This relates to the overall low toughness of the ceramics, likely larger flaw populations (cracks and pores), and limited ductility. However, the adhesive strength of metals/alloys is more subjective to the substrate chemistry and deposition temperatures. A study by Bialucki et al. (Ref 106) proved that effective removal of the alumina oxide scale from aluminum substrates enhances the adhesive strength of the interface.

Aside from the substrate alloy, coating composition and chemistry also can play an essential role in determining adhesion strength. A potential cause for the lower observed adhesion strength of thermally sprayed Ni coatings compared to Ni-5Al coatings can be attributed to the effect of coating material on the thermal state and, subsequently, adhesion strength. The Ni-5Al coatings can undergo exothermic oxidation reactions, thus yielding higher surface temperatures during thermal spraying (Ref 62). Consequentially, Ni5Al coatings under suitable processing conditions can yield better splat-substrate bonding and ultimately promote higher adhesion strength.

Unlike oxides and metals, cermets have a unique interaction with the substrates as the splats are composed of relatively dense, partially molten particles. Furthermore, in carbide-based cermets, there is the possibility for decarburization in flight which can also affect the local deposition temperature. Thus, cermets can have potential contributions from metallurgical interactions and plastic deformation to impart better adhesion between the splats and substrate. Therefore, cermets usually exhibit higher adhesion strength than ceramics and metals.

In the case of high-velocity processes such as HVOF and CS, because the residence times in the flame are so low, the melting is assumed to be minimized. So, the splat–substrate interactions are dominated by the high-velocity impact. This implies substrate deformation is the dominant adhesive mechanism. Figure 21 shows this can yield excessively high (higher than the glue) adhesion strengths with contributions from metallurgical bonding if the impact promotes bonding by breaching oxide scales.

While there is utility in such a design map for considering the fundamental characteristics of the adhesion strength of thermally sprayed coatings, this mapping approach heavily depends on the generation and analysis of highly consistent and reproducible results.

## Summary

This work is intended to serve as a comprehensive overview of the current challenges in the TAT implementation and understanding. Although in practice for over five decades, the analysis sheds light on significant inconsistencies in the test method, process dependence, and variabilities. The study breaks down operational elements concerning both testing and processing through a combination of reliable published data along with necessary in-house experiments to fill the uncertainty gaps. Some key takeaways from this study are:

- The **variability** in adhesion strength results is the major drawback of the TAT tests. Statistical analysis on an extensive data set using methods like Weibull analysis can assist in defining parameters like **Weibull modulus** and **characteristic strength** that can be used for a better understanding and/or specification purposes (i.e., establishing relevance to repeatability in coating production).

- Executing the test as per recommended guidelines established in various standards (like ASTM C633, ISO 14916, etc.) meticulously and consistently is helpful and essential to reducing site-dependent result variabilities. However, consistent testing methods do not have any significant influence in minimizing the flaw variability, and thus adhesion strength measurements via TAT are still subject to considerable scatter, especially in intrinsically brittle interfaces.
- The observed adhesion strength of an interface is a result of an interplay between three dominant aspects: the **local microstructure** (presence of defects, bonded area), **system mechanics** (elastic mismatch, modulus, flaw severity), and **splat-interface bonding mechanism** (mechanical anchorage, metallurgical bonding, plastic deformation). The contributions from these three aspects are not exclusively resolvable, as they all arise due to the inherent characteristics of the thermal spray deposition process.

- An initial framework of parametric dependencies based on a notional particle state is proposed that provides a first-order interpretation of operative mechanisms. This is subject to further refinements through modeling and significant new data generation in a controlled setting.

It is envisioned that with this review as a framework, future academic and industrial efforts can be initiated to bridge the existing knowledge gaps between TAT measurements and adhesion mechanisms. It is further necessary to develop alternative tests, especially for flaw-dominated brittle systems where the focus should be on the measurement of interface toughness rather than adhesion strength. Innovations in testing and mechanistic understanding will benefit academia and industry in pursuit of expanded thermal spray applications.

## Appendix

See Tables 4, 5 and 6

**Table 4** Grit blasting methodologies are to prepare TAT specimen prior to thermal spraying

| Average Observed Surface Roughness ($\mu$m) | Grit blasting Pressure (bar) | Grit Size Used |
|---|---|---|
| 5 | 2.75[1], 4.14[2], 5.15[3] | #24-grit $Al_2O_3$ |
| 7 | 4.14[1], 5.15[2] | #24-grit $Al_2O_3$ |
| 12 | 5.15[1,2] | #16-grit $Al_2O_3$ |

[1,2,3]Indicate aluminum, mild steel, and Inconel 718, respectively.

**Table 5** Plasma spraying parameters utilized for depositing APS coatings atop grit-blasted TAT specimen

| Spray Condition | Argon Flow Rate (slpm[*]) | Hydrogen Flow Rate (slpm[*]) | Arc Current (A) | Standoff Distance (mm) | Surface/Raster Speed (mm/s) | Particle Feed Rate (g/min) |
|---|---|---|---|---|---|---|
| F4 – Center | 47.5 | 6 | 550 | 60, 100, 150 | 500 | 30 |
| SG-100 – Center | 60* | 20[*] | 600 | 80, 100, 120 | 500 | 19.3 |

*For the SG-100 torch and AT-3000 console, the default input parameters are in psi and reported as such in this table.

Various spray distances were utilized in the experiments

**Table 6** Feedstock materials used to deposit coatings for the in-house data generated in this review

| Feedstock Material Commercial Name | Material Chemistry | Particle Morphology | Nominal Particle Size Distribution |
|---|---|---|---|
| SG204F | 7YSZ | Hollow Spherodized | 10–45 $\mu$m |
| Metco 56C-NS | 99.9% Ni | Gas Atomized | 50–105 $\mu$m |
| Metco 480-NS | Ni-5 wt.% Al | Gas Atomized | 10–60 $\mu$m |
| Metco 102 | $TiO_2$ | Spherodized | 10–60 $\mu$m |
| Praxair Al1110-HP | $Al_2O_3$ | Gas Atomized | 5–25 $\mu$m |

## Appendix: Experimental Methods for in-house Data Generation

This Appendix serves as an auxiliary resource to define all the experimental methods utilized by the authors to generate the in-house TAT reported in the article. The appendix is subdivided into two sections: A1 outlines the thermal spray process details, and A2 discusses the steps involved in TAT sample assembly and testing.

### A.1-Coating Fabrication Details

Primarily the coatings investigated via the in-house experiments were deposited via two Air Plasma Spray (APS) process setups. For the most part, an F4-HB 90 torch mounted to a six-axis robot and controlled by an A-3000S plasma spray controller was used to deposit most coatings [Oerlikon Metco, Westbury, NY]. Alternatively, an SG-100 torch using the subsonic configuration controlled by an AT-3000 thermal spray console was utilized to deposit some coatings [Thermach Inc., Appleton, WI]. Thermal spraying was carried out directly onto the TAT rod or disk substrates made of aluminum or steel (from Sect. 3.1). For a given TAT experiment, specimens were always sprayed in sets of 5, as per ASTM C633 guidelines.

Before thermal spraying, the substrates underwent a preparatory procedure to ensure the surface was ready for deposition. First, substrates were ultrasonically degreased in a solution of acetone and deionized water. Subsequently, the specimen was then grit blasted to achieve the required surface roughness. The surface roughness parameter $R_a$ was analyzed with a Mitutoyo SJ 201P stylus profilometer (Mitutoyo America, IL). Ten independent measurements were taken on a random TAT specimen from each of the freshly grit-blasted 5-sample-set, and the average $R_a$ was recorded. In some instances, coatings were sprayed directly onto as-received substrates. These substrates were only prepared by ultrasonically degreasing before thermal spraying.

The spray conditions utilized in the in-house studies were self-consistent and only varied depending on the torch and plasma spray controller used. In all cases, an argon–hydrogen plasma flame was used to heat and melt the feedstock particles to deposit the coatings. These spray conditions are outlined in Table 5. Coating thicknesses were maintained around 450-500 μm for TAT specimens unless otherwise noted.

Finally, various feedstock materials and powders were utilized to deposit coatings for the in-house studies. These powders were optimized for the thermal spray process and span a wide range of material chemistry, particle size, and morphology. The feedstocks utilized to deposit coatings are outlined in Table 6.

### A.2-TAT Specimen Assembly and Testing

After thermal spraying onto the disc/rod substrate, a TAT sample was assembled using mating substrates. Surface preparation steps (degreasing and grit blasting) for mating substrates were equivalent to the corresponding coated pieces. Before thermal spraying, it was ensured that the mating substrates had a target surface roughness $R_a$ that matched the $R_a$ of the coated specimen.

Once the mating specimen were prepared, they were glued to the coated piece. For gluing, all in-house data in this review exclusively used FM1000 polyamide wafers [Sturbridge Metallurgical Services, Inc., MA]. Gluing the coated and mating specimens was carried out using a V-block fixture, which is standard among TAT operators. The V-block fixture had pre-machined grooves for the TAT rod specimen to rest on a 30-degree incline. To clean the surfaces before gluing, the as-sprayed coating surface and the freshly grit-blasted mating specimen surface were soaked in acetone for 2–3 min. Then, an FM1000 wafer was removed from the refrigerated stock and placed on the as-sprayed coated specimen. Once aligned, the glue was sandwiched between the as-sprayed specimen and the mating piece. A 100-g mild steel 25.4 mm $\varnothing$ cylinder was placed on top of the assembly to add pressure onto the assembled TAT samples during curing. This process was repeated six times, with the sixth specimen being an FM1000 wafer sandwiched between two grit-blasted mating substrates (no coating present) as per the ASTM C633 standard. After loading the six sets of TAT specimens onto the V-block fixture with the 100-g steel weights, a threaded stud was tightened to provide a complimentary compressive force on each assembled specimen. Using a torque wrench, the studs were tightened $\sim$ 2.5 N-m to provide adequate auxiliary pressure to the FM1000 wafers.

Once the V-block fixture was fully loaded with the torqued specimens (five coated specimens, one glue test specimen), the entire fixture was placed into a temperature-controlled oven. The oven was set to hold at approximately 180 °C during operation. Once engaged, the oven remained powered for approximately 2.5 h to account for the ramp time to temperature, and adequate time at the dwell temperature for the glue to properly cure. After 2.5 h, the furnace was switched off, and the specimen in the V-block fixture was left in the oven to cure overnight.

Testing the glued TAT specimen was carried out using an Instron servo-hydraulic tensile testing machine with a static 200-kN load cell [Instron, Norwood, MA]. One glued specimen at a time was mounted to the Instron machine by

threading ½"-20 screws that connect the glued specimen to a mounting fixture and pulling the specimen along those screws. The mounting fixture incorporates universal joints so as to reduce external moments and loads applied to the system during the testing. For the TAT testing, a specialized program was written for the Instron, which initially zeroes the load cell for 45 s, then transitions to a position-controlled tensile test. Uniaxial tension was continuously applied to the system until fracture was observed, and then the machine was stopped. The recorded maximum load before fracture was stored as the critical load $P_c$, and the adhesion strength was calculated based on the load and cross-sectional area of the specimen. After testing, specimens were placed in a specially machined fixture to take photographs of the fracture surface. These photographs provided conclusive evidence of whether the failure was adhesive, cohesive, or inconclusive.

# References

1. A. Vardelle, C. Moreau, J. Akedo, H. Ashrafizadeh, C.C. Berndt, J.O. Berghaus, M. Boulos, J. Brogan, A.C. Bourtsalas and A. Dolatabadi, The 2016 Thermal Spray Roadmap, *J. Therm. Spray. Techn.*, 2016, **25**(8), p 1376–1440.

2. R. Vaßen, H. Kaßner, A. Stuke, F. Hauler, D. Hathiramani and D. Stöver, Advanced Thermal Spray Technologies for Applications in Energy Systems, *Surf. Coat. Technol.*, 2008, **202**(18), p 4432–4437.

3. R.S. Lima and B.R. Marple, Thermal Spray Coatings Engineered from Nanostructured Ceramic Agglomerated Powders for Structural, Thermal Barrier and Biomedical applIcations: A Review, *J. Therm. Spray. Techn.*, 2007, **16**(1), p 40–63.

4. P. Ernst and G. Barbezat, Thermal Spray Applications in Powertrain Contribute to the Saving of Energy and Material Resources, *Surf. Coat. Technol.*, 2008, **202**(18), p 4428–4431.

5. M.F. Smith, A.C. Hall, J.D. Fleetwood and P. Meyer, Very Low Pressure Plasma Spray—A Review of an Emerging Technology in the Thermal Spray Community, *Coatings*, 2011, **1**(2), p 117–132.

6. R. Vassen, A. Stuke and D. Stöver, Recent Developments in the Field of Thermal Barrier Coatings, *J. Therm. Spray. Techn.*, 2009, **18**(2), p 181–186.

7. U. Kogelschatz, Atmospheric-Pressure Plasma Technology, *Plasma. Phys. Contr. F*, 2004, **46**, p B63–B75. (**in English**)

8. M.R. Dorfman, Chapter 22 - Thermal Spray Coatings, Handbook of Environmental Degradation of Materials (Third Edition)ed., M. Kutz, Ed., William Andrew Publishing, 2018 p 469–488

9. D.R. Clarke, M. Oechsner and N.P. Padture, Thermal-Barrier Coatings for more Efficient Gas-Turbine Engines, *MRS Bull.*, 2012, **37**(10), p 891–902.

10. X.Q. Cao, R. Vassen and D. Stoever, Ceramic Materials for Thermal Barrier Coatings, *J. Eur. Ceram. Soc.*, 2004, **24**(1), p 1–10.

11. H. Herman, S. Sampath and R. McCune, Thermal Spray: Current Status and Future Trends, *MRS Bull.*, 2000, **25**(7), p 17–25.

12. S. Sampath, Opportunities for Thermal Spray in Functional Materials, *Electron. Sens, Adv. Mater. Process*, 2013, **171**(11), p 69–70.

13. W. Zhang, Y.-M. Guo and Y.-X. Chen, Applications and Future Development of Thermal Spraying Technologies for Remanufacturing Engineering, *Zhingguo Biaomian Gongcheng (China Surface Engineering)*, 2011, **24**(6), p 1–10.

14. G. Barbezat, Advanced Thermal Spray Technology and Coating for Lightweight Engine Blocks for the Automotive Industry, *Surf. Coat. Technol.*, 2005, **200**(5–6), p 1990–1993.

15. P.L. Fauchais, J.V. Heberlein and M.I. Boulos, Thermal Spray Fundamentals: from Powder to Part, Springer Science & Business Media, 2014

16. M.R. Dorfman, Thermal Spray Basics, *Adv. Mater. Process.*, 2002, **160**(7), p 47–51.

17. L. Pawlowski, The Science and Engineering of Thermal Spray Coatings, John Wiley & Sons, 2008

18. L.-M. Berger, Application of Hardmetals as Thermal Spray Coatings, *Int. J. Refract Metal Hard Mater.*, 2015, **49**, p 350–364.

19. E.E. Balić, M. Hadad, P.P. Bandyopadhyay and J. Michler, Fundamentals of Adhesion of Thermal Spray Coatings: Adhesion of Single Splats, *Acta Mater.*, 2009, **57**(19), p 5921–5926.

20. C.-J. Li, G.-J. Yang and C.-X. Li, Development of Particle Interface Bonding in Thermal Spray Coatings: A Review, *J. Therm. Spray. Techn.*, 2013, **22**(2–3), p 192–206.

21. G.-J. Yang, C.-X. Li, S. Hao, Y.-Z. Xing, E.-J. Yang and C.-J. Li, Critical Bonding Temperature for the Splat Bonding Formation During Plasma Spraying of Ceramic Materials, *Surf. Coat. Technol.*, 2013, **235**, p 841–847.

22. A. Rabiei and A.G. Evans, Failure Mechanisms Associated with the Thermally Grown Oxide in Plasma-Sprayed Thermal Barrier Coatings, *Acta Mater.*, 2000, **48**(15), p 3963–3976.

23. T.W. Clyne and S.C. Gill, Residual Stresses in Thermal Spray Coatings and Their Effect on Interfacial Adhesion: A Review of Recent Work, *J. Therm. Spray. Techn.*, 1996, **5**(4), p 401.

24. A.A. Volinsky, N.R. Moody and W.W. Gerberich, Interfacial Toughness Measurements for Thin Films on Substrates, *Acta Mater.*, 2002, **50**(3), p 441–466.

25. A.A. Griffith and VI., The Phenomena of Rupture and Flow in Solids, *PHILOSOPHICAL Transactions of the Royal Society of London, Series A, Containing Papers of a Math. Phys. Charac.*, 1921, **221**, p 163–198.

26. Z. Chen, K. Zhou, X. Lu and Y.C. Lam, A Review on the Mechanical Methods for Evaluating Coating Adhesion, *Acta Mech.*, 2014, **225**(2), p 431–452.

27. C.C. Berndt and C.K. Lin, Measurement of Adhesion for Thermally Sprayed Materials, *J. Adhes. Sci. Technol.*, 1993, **7**(12), p 1235–1264.

28. C.K. Lin and C.C. Berndt, Measurement and Analysis of Adhesion Strength for Thermally Sprayed Coatings, *J. Therm. Spray. Techn.*, 1994, **3**(1), p 75–104. (**in English**)

29. M. Hadad, G. Marot, P. Démarécaux, J. Lesage, J. Michler and S. Siegmann, Adhesion Tests for Thermal Spray Coatings: Application Range of Tensile, Shear and Interfacial Indentation Methods, Proceedings of ITSC, 2005, p 759

30. S. Papavinasam, M. Attard, B. Arseneult and R.W. Revie, State-of-the-Art of Thermal Spray Coatings for Corrosion Protection, **26**(2-3), 105-145 (2008)

31. K. Tani and H. Nakahira, Status of Thermal Spray Technology in Japan, *J Therm. Spray. Techn.*, 1992, **1**(4), p 333–339.

32. J. Wigren and K. Täng, Quality Considerations for the Evaluation of Thermal Spray Coatings, *J Therm Spray Techn*, 2007, **16**(4), p 533–540.

33. C.C. Berndt, Tensile Adhesion Testing Methodology for Thermally Sprayed Coatings, *J. Mater. Eng.*, 1990, **12**(2), p 151–158.

34. DIN EN ISO 14916:2017: Thermal spraying — Determination of tensile adhesive strength, *International Organization for Standardization*, **ICS.25.220.20**, 26 (2017)

35. ASTM C633–13(2021): Standard Test Method for Adhesion or Cohesion Strength of Thermal Spray Coatings, *ASTM International*, (2021)

36. K. Mittal, STP640-EB: Adhesion Measurement of Thin Films, Thick Films, and Bulk Coatings, ASTM International, (1978)

37. A91–202–79 AFNOR NF: "Characteristics and Methods of Test for Metal Spraying", *Association Francaise de Normalisation*, (1979)

38. DIN 50 160: "Determination of Adhesive Strength in the Traction-Adhesive Strength Test", *German institute for standardisation*, (1981)

39. J.S. Association, JIS H 8666:1994: " Test Methods for Ceramic Sprayed Coatings", *Japanese Industrial Standards (JIS)*, (1994)

40. G. Fehringer, S. Janes, M. Wildersohn and R. Clasen, Proton—Conducting Ceramics as Electrode/Electrolyte—Materials for SOFCs: Preparation, Mechanical and Thermal-Mechanical Properties of Thermal Sprayed Coatings, Material Combination and Stacks, *J. Eur. Ceram. Soc.*, 2004, **24**(5), p 705–715.

41. W. Funk and F. Goebe, Bond Strength Optimization of Plasma-Sprayed Cr2O3 Layers by Factorial Two-Level Experiments, *Thin Solid Films*, 1985, **128**(1), p 45–55.

42. JIS H 8402: Test Methods of Tensile Adhesive Strength for Thermal-Sprayed Coatings, *Japanese Standards Association (JSA)*, (2019)

43. R. Apps, The Influence of Surface Preparation on The Bond Strength of Flame-Sprayed Aluminium Coatings on Mild Steel, *J. Vac. Sci. Technol.*, 1974, **11**(4), p 741–746.

44. E. Bardal, P. Molde and T. Eggen, Arc and Flame Sprayed Aluminium and Zinc Coatings on Mild Steel: Bond Strength, Surface Roughness, Structure and Hardness, *Br. Corros. J.*, 1973, **8**(1), p 15–19.

45. R.F. Brown, G.M. Smith, A. Hehr and T.J. Eden, Ultrasonic Consolidation Post-Treatment of CuNi: Cr3C2-NiCr Composite Cold Spray Coatings: A Mechanical and Microstructure Assessment, *J Therm Spray Techn*, 1–14 (2021)

46. S. Dosta, M. Couto and J. Guilemany, Cold Spray Deposition of a WC-25Co Cermet onto Al7075-T6 and Carbon Steel Substrates, *Acta Mater.*, 2013, **61**(2), p 643–652.

47. J. Guilemany, J. Nutting, V. Sobolev, Z. Dong, J. De Paco, J. Calero and J. Fernandez, Interface Structures of High Velocity Oxy-Fuel Sprayed WC-Co Coating on a Copper Substrate, *Mater. Sci. Eng., A*, 1997, **232**(1–2), p 119–128.

48. C. Lyphout, P. Nylen and L.G. Östergren, Adhesion Strength of HVOF Sprayed IN718 Coatings, *J. Therm. Spray. Techn.*, 2012, **21**(1), p 86–95.

49. M.H. Staia, E. Ramos, A. Carrasquero, A. Roman, J. Lesage, D. Chicot and G. Mesmacque, Effect of Substrate Roughness Induced by Grit Blasting Upon Adhesion of WC-17% Co Thermal Sprayed Coatings, *Thin Solid Films*, 2000, **377–378**, p 657–664.

50. G.-J. Yang, C.-J. Li, C.-X. Li, K. Kondoh and A. Ohmori, Improvement of Adhesion and Cohesion in Plasma-Sprayed Ceramic Coatings by Heterogeneous Modification of Non-bonded Lamellar Interface using High Strength Adhesive Infiltration, *J. Therm. Spray. Techn.*, 2013, **22**(1), p 36–47.

51. Technical Data Sheet: "FM 1000 Adhesive Film", (Solvay ) https://www.e-aircraftsupply.com/MSDS/83119FM-1000.pdf (Accessed Dec 09, 2021)

52. S.H. Leigh and C.C. Berndt, A Test for Coating Adhesion on Flat Substrates—a Technical Note, *J. Therm. Spray. Techn.*, 1994, **3**(2), p 184–190.

53. S.H. Leigh, C.C. Berndt, C.L. Wu and T. Nakamura, Tensile adhesion testing of thermal spray coatings on flat substrates, ASM International, 1994

54. W. Han, E. Rybicki and J. Shadley, An Improved Specimen Geometry for ASTM C633–79 to Estimate Bond Strengths of Thermal Spray Coatings, *J. Therm. Spray. Techn.*, 1993, **2**(2), p 145–150.

55. W. Han, E. Rybicki and J. Shadley, Application of Fracture Mechanics to the Interpretation of Bond Strength Data from ASTM Standard C633–79, *J. Therm. Spray. Techn.*, 1993, **2**(3), p 235–241.

56. Accepted Practice to Test Bond Strength of Thermal Spray Coatings, J Therm Spray Techn, **22**(8), 1263–1266 (2013)

57. W. Weibull, A statistical theory of strength of materials, *IVB-Handl.*, (1939)

58. B. Basu, D. Tiwari, D. Kundu and R. Prasad, Is Weibull Distribution the Most Appropriate Statistical Strength Distribution for Brittle Materials?, *Ceram. Int.*, 2009, **35**(1), p 237–246.

59. K. Evans, Tensile Bond Strength Variance of Thermally Sprayed Coatings with Respect to Adhesive Type, ITSC 1996, 1996, ASM International, pp 803–806

60. C.R.C. Lima and J.M. Guilemany, Adhesion Improvements of Thermal Barrier Coatings with HVOF Thermally Sprayed Bond Coats, *Surf. Coat. Tech.*, 2007, **201**, p 4694.

61. C. Lyphout, P. Nylén and L. Östergren, Relationships Between Process Parameters, Microstructure, and Adhesion Strength of HVOF Sprayed IN718 Coatings, *J. Therm. Spray. Techn.*, 2011, **20**(1), p 76–82.

62. S. Sampath, X.Y. Jiang, J. Matejicek, L. Prchlik, A. Kulkarni and A. Vaidya, Role of Thermal Spray Processing Method on the Microstructure, Residual Stress and Properties of Coatings: an Integrated Study for Ni-5 wt.%Al Bond Coats, *Mat. Sci. Eng. a-Struct.*, 2004, **364**, p 216–231.

63. A. Nusair Khan, J. Lu and H. Liao, Effect of Residual Stresses on Air Plasma Sprayed Thermal Barrier Coatings, *Surf. Coat. Techn.*, 2003, **168**(2), p 291–299.

64. B.E. 582, "Thermal Spraying - Determination of Tensile Adhesive Strength," British Standards Institution (BSI) 1994

65. S.V. Shinde, E.J. Gildersleeve, C.A. Johnson and S. Sampath, Segmentation Crack Formation Dynamics during Air Plasma Spraying of Zirconia, *Acta Mater.*, 2020, **183**, p 196–206.

66. S.V. Shinde and S. Sampath, Factors Governing Segmentation Crack Characteristics in Air Plasma Sprayed Ceramics, *J. Eur. Ceram. Soc.*, 2022, **42**(3), p 1077–1087.

67. C.A. Brown and S. Siegmann, Fundamental Scales of Adhesion and Area–Scale Fractal Analysis, *Int. J. Mach. Tools Manuf*, 2001, **41**(13–14), p 1927–1933.

68. S. Siegmann, C. Brown, Surface Texture Correlations with Tensile Adhesive Strength of Thermally Sprayed Coatings using Area-Scale Fractal Analysis, United Thermal Spray Conference–Proceedings, E. Lugschneider, PA Kammer, eds., DVS Verlag, Dusseldorf, 1999, pp 355–359

69. M. Lance, B.P. Thiesing, J.A. Haynes, E.J. Gildersleeve, S. Sampath and B.A. Pint, Effect of APS Flash Bond Coatings and Curvature on TBC Performance on Rod Specimens, *Surf. Coat. Technol.*, 2019, **378**, 124940.

70. M. Hadad, G. Marot, J. Lesage, J. Michler and S. Siegmann, Adhesion Tests for Thermal Spray Coatings: Application Range of Tensile, Shear and Interfacial Indentation Methods, 2005

71. G. Dwivedi, V. Viswanathan, S. Sampath, A. Shyam and E. Lara-Curzio, Fracture Toughness of Plasma-Sprayed Thermal Barrier Ceramics: Influence of Processing, *Microstruct. Therm.*

*Aging, J. Am. Ceram Soc.*, 2014, **97**(9), p 2736–2744. (**in English**)

72. N. Cinca and J.M. Guilemany, Thermal Spraying of Transition Metal Aluminides: An Overview, *Intermetallics*, 2012, **24**, p 60–72.

73. N. Cinca, C.R.C. Lima and J.M. Guilemany, An Overview of Intermetallics Research and Application: Status of Thermal Spray Coatings, *J. Market. Res.*, 2013, **2**(1), p 75–86.

74. L.A. Giannuzzi, N.S. Smith and S. Sampath, Characterization of Coatings with Ions and Electrons, *Microsc. Microanal.*, 2013, **19**(S2), p 1862–1863.

75. Y. Wu, M. Qu, L.A. Giannuzzi, S. Sampath and A. Gouldstone, Focused Ion Beam Study of Ni5Al Single Splat Microstructure, *MRS Online Proceedings Library (OPL)*, **983**, (2006)

76. X. Luo, G.M. Smith and S. Sampath, On the Interplay Between Adhesion Strength and Tensile Properties of Thermal Spray Coated Laminates—Part I: High Velocity Thermal Spray Coatings, *J. Therm. Spray. Techn.*, 2018, **27**(3), p 296–307.

77. X. Luo, G.M. Smith and S. Sampath, On the Interplay Between Adhesion Strength and Tensile Properties of Thermal Spray Coated Laminates—Part II: Low-Velocity Thermal Spray Coatings, *J. Therm. Spray. Techn.*, 2018, **27**(3), p 308–318.

78. G.M. Smith, Mechanical Properties of Thermal Spray Coatings and Systems, State University of New York at Stony Brook, 2018

79. D. Greving, J. Shadley and E. Rybicki, Effects of Coating Thickness and Residual Stresses on the Bond Strength of ASTM C633–79 Thermal Spray Coating Test Specimens, *J. Therm. Spray. Techn.*, 1994, **3**(4), p 371.

80. C.-J. Li and Y.-Y. Wang, Effect of Particle State on the Adhesive Strength of HVOF Sprayed Metallic Coating, *J. Therm. Spray. Techn.*, 2002, **11**(4), p 523–529.

81. Y.Y. Wang, C.J. Li and A. Ohmori, Influence of Substrate Roughness on the Bonding Mechanisms of High Velocity Oxy-Fuel Sprayed Coatings, *Thin Solid Films*, 2005, **485**(1), p 141–147.

82. H. Fukanuma and N. Ohno, Influences of Substrate Roughness and Temperature on Adhesive Strength in Thermal Spray Coatings, *Proceedings of Thermal Spray 2003: Advancing the Science & Applying the Technology*, (2003)

83. V. Pershin, M. Lufitha, S. Chandra and J. Mostaghimi, Effect of Substrate Temperature on Adhesion Strength of Plasma-Sprayed Nickel Coatings, *J. Therm. Spray. Techn.*, 2003, **12**(3), p 370–376.

84. Y. Watanabe, C. Yoshida, K. Atsumi, M. Yamada and M. Fukumoto, Influence of Substrate Temperature on Adhesion Strength of Cold-Sprayed Coatings, *J. Therm. Spray. Techn.*, 2015, **24**(1–2), p 86–91.

85. T. Arai, H. Fujita and M. Watanabe, Evaluation of Adhesion Strength of Thin Hard Coatings, *Thin Solid Films*, 1987, **154**(1–2), p 387–401.

86. P. Araujo, D. Chicot, M. Staia and J. Lesage, Residual Stresses and Adhesion of Thermal Spray Coatings, *Surf. Eng.*, 2005, **21**(1), p 35–40.

87. M. Othman, A. Bushroa and W.N.R. Abdullah, Evaluation Techniques and Improvements of Adhesion Strength for TiN Coating in Tool Applications: A Review, *J. Adhes. Sci. Technol.*, 2015, **29**(7), p 569–591.

88. R. Singh, S. Schruefer, S. Wilson, J. Gibmeier and R. Vassen, Influence of Coating Thickness on Residual Stress and Adhesion-Strength of Cold-Sprayed Inconel 718 Coatings, *Surf. Coat. Technol.*, 2018, **350**, p 64–73.

89. E.J. Gildersleeve V and S. Sampath, Process-Geometry Interplay in the Deposition and Microstructural Evolution of 7YSZ Thermal Barrier Coatings by Air Plasma Spray, *J Therm Spray Techn*, **29**(4), (2020)

90. J.W. Hutchinson and Z. Suo, Mixed Mode Cracking in Layered Materials, Advances in Applied Mechanics Volume 29ed., 1991, p 63–191

91. G. Qian, T. Nakamura, C.C. Berndt and S.H. Leigh, Tensile Toughness Test and High Temperature Fracture Analysis of Thermal Barrier Coatings, *Acta Mater.*, 1997, **45**(4), p 1767–1784. (**in English**)

92. Y. Okajima, T. Nakamura and S. Sampath, Effect of Powder Injection on the Interfacial Fracture Toughness of Plasma-Sprayed Zirconia, *J. Therm. Spray. Techn.*, 2013, **22**(2–3), p 166–174. (**in English**)

93. Y. Okajima, T. Nakamura and S. Sampath, Interfacial Fracture Toughness and Residual Stress of Thermally Sprayed Coatings, *Exp. Appl. Mech.*, 2013, **4**, p 285–292.

94. S. Chen, S. Liu, Y. Wang, X. Sun, Z. Zou, X. Li and C. Wang, Microstructure and Properties of HVOF-Sprayed NiCrAlY Coatings Modified by Rare Earth, *J. Therm. Spray. Techn.*, 2014, **23**(5), p 809–817.

95. V. Higuera Hidalgo, J. Belzunce Varela, A. Carriles Menendez and S. Poveda Martínez, High Temperature Erosion Wear of Flame and Plasma-Sprayed Nickel–Chromium Coatings under Simulated Coal-Fired Boiler Atmospheres, *Wear*, 2001, **247**(2), p 214–222.

96. B. Li, J. Jia, Y. Gao, M. Han and W. Wang, Microstructural and Tribological Characterization of NiAl Matrix Self-Lubricating Composite Coatings by Atmospheric Plasma Spraying, *Tribol. Int.*, 2017, **109**, p 563–570.

97. H. Masoumi, S.M. Safavi, M. Salehi and S.M. Nahvi, Effect of Grinding on the Residual Stress and Adhesion Strength of HVOF Thermally Sprayed WC–10Co–4Cr Coating, *Mater. Manuf. Process.*, 2014, **29**(9), p 1139–1151.

98. G. Matache, C. Puscasu, A. Paraschiv and O. Trusca, Investigation of Some Intrinsic Properties of Thermal Sprayed Molybdenum Coatings for Railway Axle Applications, *Appl. Mech. Mater.*, 2015, **811**, p 19–23.

99. M. Mellali, P. Fauchais and A. Grimaud, Influence of Substrate Roughness and Temperature on the Adhesion/Cohesion of Alumina Coatings, *Surf. Coat. Technol.*, 1996, **81**(2), p 275–286.

100. S. Tailor, A. Modi and S.C. Modi, High-Performance Molybdenum Coating by Wire–HVOF Thermal Spray Process, *J. Therm. Spray. Techn.*, 2018, **27**(4), p 757–768.

101. C. Thiruvikraman, V. Balasubramanian and K. Sridhar, Optimizing HVOF Spray Parameters to Maximize Bonding Strength of WC-CrC-Ni Coatings on AISI 304L Stainless Steel, *J. Therm. Spray. Techn.*, 2014, **23**(5), p 860–875.

102. E. Turunen, T. Varis, S.P. Hannula, A. Vaidya, A. Kulkarni, J. Gutleber, S. Sampath and H. Herman, On the Role of Particle State and Deposition Procedure on Mechanical, Tribological and Dielectric Response of High Velocity Oxy-Fuel Sprayed Alumina Coatings, *Mater. Sci. Eng., A*, 2006, **415**(1), p 1–11.

103. P. Varghese, E. Vetrivendan, R. Krishnan, T. Mathews and S. Ningshen, Plasma Sprayed Alumina-Yttria Composite Ceramic Coating for Electrical Insulation Applications, *Surf. Coat. Technol.*, 2021, **405**, 126566.

104. M. Vijaya Babu, R. Krishna Kumar, O. Prabhakar and N. Gowri Shankar, Fracture Mechanics Approaches to Coating Strength Evaluation, *Eng. Fract. Mech.*, 1996, **55**(2), p 235–248.

105. J. Yan, Z. He, Y. Wang, J. Qiu and Y. Wang, Microstructure and Wear Resistance of Plasma-Sprayed Molybdenum Coating Reinforced by MoSi2 Particles, *J. Therm. Spray. Techn.*, 2016, **25**(7), p 1322–1329.

106. P. Białucki and S. Kozerski, Study of Adhesion of Different Plasma-Sprayed Coatings to Aluminium, *Surf. Coat. Technol.*, 2006, **201**(5), p 2061–2064.